Accepted Manuscript

A new exploration towards aminothiazolquinolone oximes as potentially multi-targeting antibacterial agents: Design, synthesis and evaluation acting on microbes, DNA, HSA and topoisomerase IV

Liang-Liang Wang, Narsaiah Battini, Rammohan R. Yadav Bheemanaboina, Mohammad Fawad Ansari, Jin-Ping Chen, Yun-Peng Xie, Gui-Xin Cai, Shao-Lin Zhang, Cheng-He Zhou

PII: S0223-5234(19)30573-2

DOI: https://doi.org/10.1016/j.ejmech.2019.06.046

Reference: EJMECH 11449

To appear in: *European Journal of Medicinal Chemistry*

Received Date: 30 March 2019

Revised Date: 15 June 2019

Accepted Date: 16 June 2019

Please cite this article as: L.-L. Wang, N. Battini, R.R. Yadav Bheemanaboina, M.F. Ansari, J.-P. Chen, Y.-P. Xie, G.-X. Cai, S.-L. Zhang, C.-H. Zhou, A new exploration towards aminothiazolquinolone oximes as potentially multi-targeting antibacterial agents: Design, synthesis and evaluation acting on microbes, DNA, HSA and topoisomerase IV, *European Journal of Medicinal Chemistry* (2019), doi: https://doi.org/10.1016/j.ejmech.2019.06.046.

Graphical Abstract

A new exploration towards aminothiazolquinolone oximes as potentially multi-targeting antibacterial agents: Design, synthesis and evaluation acting on microbes, DNA, HSA and topoisomerase IV

Liang-Liang Wang[1], Narsaiah Battini[1,†], Rammohan R. Yadav Bheemanaboina[1,†], Mohammad Fawad Ansari[1,‡], Jin-Ping Chen[1], Yun-Peng Xie[1], Gui-Xin Cai[1,*], Shao-Lin Zhang[2,*], Cheng-He Zhou[1,*]

[1] *Institute of Bioorganic & Medicinal Chemistry, Key Laboratory of Applied Chemistry of Chongqing Municipality, School of Chemistry and Chemical Engineering, Southwest University, Chongqing 400715, P. R. China.*

[2] *School of Pharmaceutical Sciences, Chongqing Key Laboratory of Natural Product Synthesis and Drug Research, Chongqing University, Chongqing, 401331, P. R. China.*

† Postdoctoral researchers from CSIR-Indian Institute of Integrative Medicine (IIIM), India

‡ Postdoctoral researcher from Jamia Millia Islamia, India.

* Corresponding Address:

Tel.: +86-23-68254967; fax: +86-23-68254967; E-mail: gxcai@swu.edu.cn (Gui-Xin Cai); zhangsl@cqu.edu.cn (Shao-Lin Zhang); zhouch@swu.edu.cn (Cheng-He Zhou).

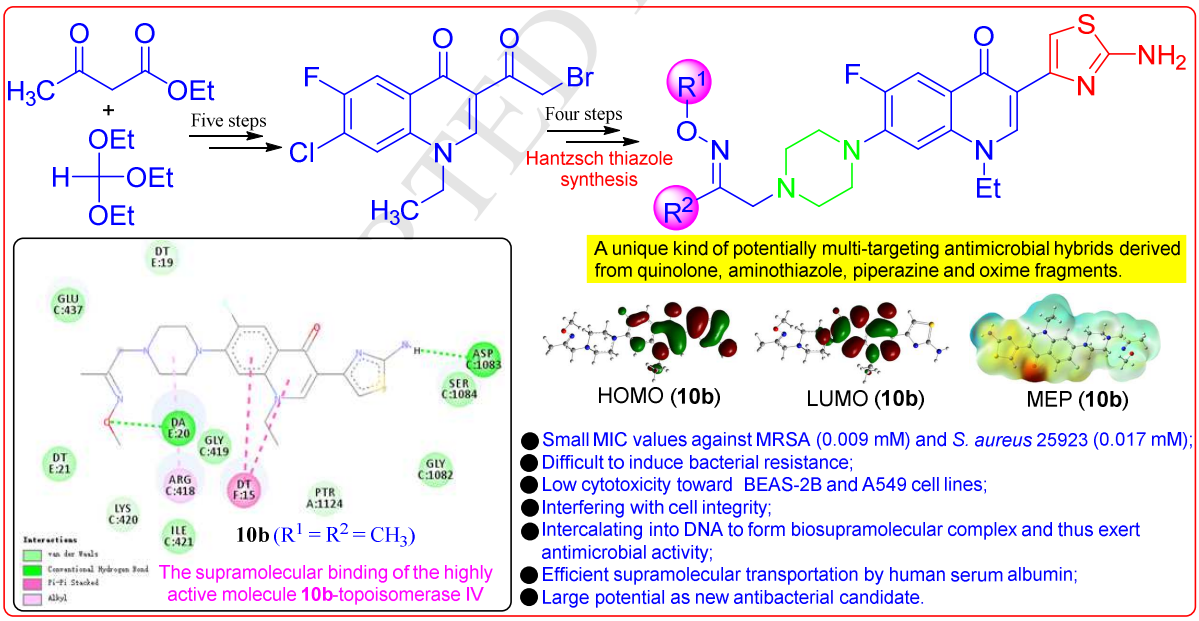

Title page

Title:

A new exploration towards aminothiazolquinolone oximes as potentially multi-targeting antibacterial agents: Design, synthesis and evaluation acting on microbes, DNA, HSA and topoisomerase IV

Author Names and Affiliations:

Liang-Liang Wang[1], Narsaiah Battini[1,†], Rammohan R. Yadav Bheemanaboina[1,†], Mohammad Fawad Ansari[1,‡], Jin-Ping Chen[1], Yun-Peng Xie[1], Gui-Xin Cai[1,*], Shao-Lin Zhang[2,*], Cheng-He Zhou[1,*]

[1] *Institute of Bioorganic & Medicinal Chemistry, Key Laboratory of Applied Chemistry of Chongqing Municipality, School of Chemistry and Chemical Engineering, Southwest University, Chongqing 400715, P. R. China.*

[2] *School of Pharmaceutical Sciences, Chongqing Key Laboratory of Natural Product Synthesis and Drug Research, Chongqing University, Chongqing, 401331, P. R. China.*

[†] Postdoctoral researchers from CSIR-Indian Institute of Integrative Medicine (IIIM), India.

[‡] Postdoctoral researcher from Jamia Millia Islamia, India.

[*] Corresponding Address:

Tel.: +86-23-68254967; fax: +86-23-68254967; gxcai@swu.edu.cn (Gui-Xin Cai); zhangsl@cqu.edu.cn (Shao-Lin Zhang); zhouch@swu.edu.cn (Cheng-He Zhou).

Abstract:

This work did a new exploration towards aminothiazolquinolone oximes as potentially multi-targeting antimicrobial agents. A class of novel hybrids of quinolone, aminothiazole, piperazine and oxime fragments were designed for the first time, conveniently synthesized as well as characterized by ^{1}H NMR, ^{13}C NMR and HRMS spectra. Biological activity showed that some of the synthesized compounds exhibited good antimicrobial activities in comparison with the reference drugs. Especially, *O*-methyl oxime derivative **10b** displayed excellent inhibitory efficacy against MRSA and *S. aureus* 25923 with MIC values of 0.009 and 0.017 mM, respectively. Further studies indicated that the highly active compound **10b** showed low toxicity toward BEAS-2B and A549 cell lines and no obvious propensity to trigger the development of bacterial

resistance. Quantum chemical studies have also been conducted and rationally explained the structural features essential for activity. The preliminarily mechanism exploration revealed that compound **10b** could not only exert efficient membrane permeability by interfering with the integrity of cells, bind with topoisomerase IV–DNA complex through hydrogen bonds and π-π stacking, but also form a steady biosupramolecular complex by intercalating into DNA to exert the efficient antibacterial activity. The supramolecular interaction between compound **10b** and human serum albumin (HSA) was a static quenching, and the binding process was spontaneous, where hydrogen bonds and Van der Waals force played vital roles in the supramolecular transportation of the active compound **10b** by HSA.

***Keywords*:**

Quinolone; Oxime; Thiazole; Antimicrobial; Molecular docking.

1. Introduction

Quinolones are one of the most important first-line antibacterial agents with high oral bioavailability, good pharmacokinetic properties and excellent curative effects, which have been employed as an effective weapon to struggle against morbidity and mortality caused by microbial pathogens [1]. This kind of drugs could target DNA gyrase or topoisomerase IV by binding with the enzyme–DNA binary complexes *via* a water-metal ion bridge to trigger irrepairable DNA breakage, interfering DNA replication and ultimately bringing about bacterial cell death [2]. However, due to the excessive use and even abuse of this kind of drugs in clinical therapy, the resistance of pathogenic bacteria is increasing seriously, and some serious side effects like gastroenteritis, vomiting and cartilage damage also have gradually emerged, which have brought great challenge for public health, underscoring the need to develop more effective new quinolone derivatives with profound potentiality to overcome the side effects and drug-resistance [3]. In recent years, the chemical modification on quinolone skeleton by various types of medicinally important structural fragments has attracted great attention and led to a large number of new marketed quinolone-based antibacterial agents with excellent antibacterial activity and pharmacokinetic profiles [4].

It has been found that the structural modification at C-3, C-6 or C-7 positions of the quinolone ring is generally the most essential and efficient strategy [5]. It was considered that the carboxyl group of C-3 position was related to the side-effects of the quinolone [6], which might be attributed to the conjugation of the benzopyridone skeleton to the carboxyl moiety to some extent. Therefore, the substitution of the carboxyl group at the C-3 position by other isosteric groups might be a promising alternative pathway to change the classic binding mode of quinolone to the enzyme–DNA complex, and eventually reduce or overcome the resistance as well as the side effects [7]. In addition, the modification of the C-6 and C-7 positions also has a significant effect on the biological and pharmacological properties of quinolones, especially the substitution at the C-7 position could greatly affect the inhibitory activity of topoisomerase and cell membrane permeabilization, and ultimately impact the solubility, bioactivity, and pharmacokinetics [8]. These strongly promoted much effort to focus on the structural modification of these sites in the quinolone ring by incorporating various types of functional fragments.

Azoles are five-membered nitrogen-containing heterocyclic compounds that played an important role in the field of medicinal chemistry [9], particularly azole-based antimicrobial agents [10]. The incorporation of azole rings into quinolone has resulted in the discovery of lots of quinolone-based azoles derivatives with strong bioactivity and high safety profile [11]. Aminothiazole as the most representative azole has been attracting interest of medicinal chemists in drug development due to its unique structure with five-membered aromatic heterocyclic core containing nitrogen and sulfur atoms, which make its derivatives possess good binding ability to interact with their functional targets [12]. The hybridization of weakly basic 2-aminothiazole fragment with quinolones might be a rationale choice to construct more effective candidates.

Oxime group (-C=N-O-) is an important fragment in antimicrobial drugs like cefodizime, cefoselis and cefmenoxime (antibacterial) as well as oxiconazole (antifungal), which was characterized with both electron accepting group (C=N) and donating group (-O-), could easily bind with various biomolecules like nucleic acid DNA, RNA, or some important enzymes through non-covalent interactions [13]. In addition, the introduction of oxime fragments into quinolone led to the discovery of quinolone oxime derivatives [14], most of them showed excellent antibacterial potentiality and pharmacokinetic characteristics, which further emphasized the importance of the oxime fragments with respect to biological activity [15], therefore, the structural modification of oximes toward quinolone is still an attractive topic.

Piperazine ring is a beneficial structural fragment for bioactivity because of its unique structure that can easily form hydrogen bonds or ionic bonds to regulate the lipid-water partition coefficient (log*P*) and acid-base balance constant of drugs, and prevalently presents in a large variety of potent marketed antimicrobial drugs like linezolid and ciprofloxacin [16]. Much work has shown that the incorporation of a functionalized polar alkaline piperazinyl group into quinolone not only significantly improves the water solubility but also is helpful for enhancing the antibacterial activity [5]. Furthermore, considering that the piperazine moiety possesses enough structural flexibility for product optimization, it is typically used as an attractive linker to develop more innovative multi-functional quinolone hybrids with better biological activities, bioavailability and lower toxicity [17].

Considering all the above facts and in continuation of our previous works on the development of 2-aminothiazolyl quinolones [18], here we reported the design, synthesis and biological activity of a class of novel hybrids of quinolone, aminothiazole, piperazine and oxime fragments, in which the acidic carboxyl group at the C-3 position was replaced by a weak basic 2-aminothiazole moiety as an isosteric group, and various functional oxime fragments were incorporated into the C-6 or C-7 positions of the quinolone ring through a piperazine bridge (Fig. 1). This series of new multi-component hybrids might possess multi-targeting antibacterial potentiality. Thus a series of piperazine-bridged aminothiazolquinolone oximes with various substituents were prepared, and their chemical structures were characterized by ^{1}H NMR, ^{13}C NMR and HRMS spectra. All the synthesized aminothiazolquinolone oximes were evaluated for their antimicrobial ability. The highly active compounds were also investigated for the cytotoxic activity, bacterial resistance and drug combination use. Furthermore, the possible antibacterial mechanism was preliminarily explored, including biofilm disruption assay, molecular docking and biosupramolecular interactions with DNA. Additionally, the ability evaluation for the supramolecular transportation of the active compound by human serum albumin (HSA) was performed to study its absorption, distribution and metabolism.

Fig. 1

2. Results and discussion

2.1. Chemistry

The synthetic routes for the desired series of C-6 or C-7 substituted aminothiazolquinolone oximes **10a-c**, **11**, **15a-e**, **22a-b**, **23a-d** and imine derivative **10d** were shown in Schemes 1–3. First, the ethyl 2-(ethoxymethylene)-3-oxobutanoate **2** was obtained from the condensation of commercial triethoxymethane **1**, ethyl acetoacetate and acetic anhydride, further reacted with 3-chloro-4-fluoroaniline and then cyclized in phenoxybenzene under reflux to give the 3-acetyl quinolone derivative **4** in 53.3% yield. The prepared intermediate **4** went through *N*-alkylation by bromoethane in acetonitrile, bromination *via* bromine in acetic acid and then cyclization with thiourea in ethanol to afford aminothiazolyl quinolone derivative **7** in 70.9% yield. The substitution of the chlorine atom at the C-7 position of 2-aminothiazolyl quinolone **7** with piperazine in NMP at 125 ºC under nitrogen atmosphere produced the 7-piperazine-substituted quinolone **8** with the yield of 33.2%. The piperazine derivative **8** was further reacted with 1-chloropropan-2-one to get the corresponding carbonyl compound **9** in 65.3% yield. The oximation of the carbonyl derivative **9** with a series of alkoxyamines in acetonitrile at 80 ºC with potassium carbonate as base produced the corresponding oximes **10a-c** with moderate to good yields ranging from 56.5% to 67.3%. Under similar conditions, the imine compound **10d** was also obtained in 52.6% yield. The oxime derivative **10a** was further modified by 2,4-dichlorobenzyl chloride to yield the target compound **11** in 50.9% yield (Scheme 1).

Scheme 1

The 7-substituted quinolone oximes **15a-e** were synthesized according to Scheme 2. The desired intermediates **13a-e** were efficiently prepared by the acetylation of substituted benzenes **12a-e** with chloroacetyl chloride at room temperature for 20 h, and further subjected to condensation with *O*-methylhydroxylamine hydrochloride in ethanol to afford various phenyl substituted *O*-methyloxime intermediates **14a-e** in moderate yields of 50.4–70.1%. Subsequently, the desired 7-substituted oxime derivatives **15a-e** were conveniently prepared by the *N*-alkylation of quinolone derivative **8** with various phenyl substituted *O*-methyloximes **14a-e** with yields ranging from 54.6% to 60.4%.

Scheme 2

With the aim to investigate the effect of different substituted oxime fragments at the C-6 position of quinolone skeleton on antimicrobial activity, a set of 6-substituted quinolone oxime derivatives **22a-b** and phenyl oximes **23a-d** were synthesized by directly coupling with piperazine moiety at C-6 position of quinolone as shown in Scheme 3. The nucleophilic aromatic substitution of intermediate **5** with the piperazinyl moiety in DMSO at 140 ºC using triethylamine as base gave 6-substituted quinolone **16** and 7-substituted quinolone by-product with 41.7 and 55.1% yields, respectively. The 6-substituted derivative **16** was protected by Boc group, and the product was brominated with cupric bromide in ethyl acetate to yield corresponding 3-(2,2-dibromoacetyl)quinolone **18** in 50.1% yield. Subsequent cyclization with thiourea in ethanol afforded 6-substituted 3-aminothiazolquinolone **19**, which was further removed the Boc group to produce the desired compound **20**. A similar procedure described for the synthesis of compounds

10a-d, was used for the preparation of target molecules **22a-b** starting from intermediate **20**. Compound **20** was reacted with 1-chloropropan-2-one and then condensed with hydroxylamine hydrochloride or *O*-methylhydroxylamine hydrochloride to generate target compounds **22a-b** in 54.2–61.8% yields. The target 6-substituted oxime derivatives **23a–d** were efficiently prepared from the reaction of the intermediate **20** and phenyl *O*-methyl oximes **14a-d** with yields ranging from 59.0% to 63.7%.

Scheme 3

2.1.1. The mechanism for the construction of thiazole ring.

The plausible mechanism for the construction of thiazole ring takes place *via* the Hantzsch thiazole synthesis, the thiazole derivative (**E**) was formed by condensation of *α*-haloketone or *α*-dihaloketone (**A**) and thiourea (**B_1**). This reaction occurs because of the thiourea as tautomer (**B_2**) and forms an intermediate (**C**). The intermediate (**C**) undergoes intramolecular cyclization to form a five-membered cyclic intermediate (**D**), followed by dehydration/elimination of bromic acid of cyclic intermediate (**D**) to give final molecule (**E**) (Scheme 4).

Scheme 4

2.1.2. Analysis of configuration (E or Z)

There are usually two configurations of oxime fragment, *Z* and *E*, so it was necessary to identify the geometries of the target oxime derivatives. Therefore, the single crystal of oxime derivative **22b** was obtained and X-ray diffraction analysis showed that the oxime geometry was *E* configuration (Fig. 2 and Fig. S1). This is because the *Z* configuration is generally unstable and easily converted to the *E* configuration. Furthermore, the NOE experiment with final compound (**15b)** was also performed to confirm the configuration but no correlation was observed between the crucial protons of $–OCH_3$ and *N*–CH_2 and the results revealed that the oxime geometry should possess similar configuration to compound **22b** (Supplementary NOESY spectrum).

Fig. 2

2.2. Biological Activity

All the synthesized aminothiazolquinolone oxime derivatives were evaluated for their *in vitro* antibacterial and antifungal activities according to Clinical and Laboratory Standards Institute (CLSI) by means of the two folds serial dilution technique, and the clinical drug chloromycin, norfloxacin and fluconazole were used as the positive controls [19]. The minimum inhibitory concentration (MIC) is defined as the lowest concentration (mM) of target molecules that could completely inhibit the growth of bacteria or fungi. The antibacterial and antifungal data were summarized in Table 1 and Table S1.

2.2.1. Antibacterial activity

The *in vitro* antibacterial evaluation in Table 1 demonstrated that some of the prepared oxime derivatives exhibited good inhibitory activity against the tested strains. Especially, 7-substituted quinolone oxime derivative **10b** not only displayed broad antibacterial spectrum among all the tested strains, but also could effectively inhibit the growth of the MRSA strain with low MIC value of 0.009 mM, which was 5-fold and 2-fold more potent than the positive controls of chloromycin (0.050 mM) and norfloxacin (0.025 mM). However, the structure–activity relationship (SAR) data revealed that the methoxy fragment of oxime derivative **10b** was replaced by hydroxy or ethoxy group, the corresponding hydroxy and ethoxy derivatives **10a** and **10c** gave moderate MIC values in the range of 0.034–0.288 mM showing relatively weak biological activity in comparison with compound **10b**, which indicated that either decrease or increase of the alkyl chain length of the alkoxy fragment could not effectively improve their biological activity. In addition, we have also found if the alkyl group of the oxime fragment was substituted by the 2,4-dichlorobenzyl group, the resulting compound **11** also significantly lose its biological activity. To further investigate the effect of oxime fragments on the biological activity of this class of compounds, the *O*-methyl oxime was substituted with semicarbazide to afford corresponding imine derivative **10d**. Although it showed a broad spectrum of antibacterial activity, the biological activity was significantly reduced. After direct comparison of the activities of compounds **9** and **10b**, it was also found that for most of the tested strains, the biological activity of *O*-methyl oxime derivative **10b** was significantly better than that of carbonyl derivative **9**. These results indicated that the oxime fragment played an important role in the antibacterial activity, especially the introduction of the *O*-methyl oxime fragment could greatly optimize the biological activity.

Table 1

Much research has reported that halogen-containing phenyl moieties are beneficial for biological activity and membrane permeability and could exert large effect on the rate of absorption and transport of drugs [20]. In our work, with the aim to enrich the chemical diversity as well as to further explore the SAR, a series of halogenated phenyl *O*-methyl oximes **15a-e** were synthesized and evaluated for their antibacterial activities. Among them, the 4-chlorophenyl-*O*-methyl oxime derivative **15b** exhibited the best activities against the tested bacteria with MIC values ranging from 0.029 to 0.461 mM. Especially, it could effectively inhibit the growth of MRSA strain with MIC value of 0.029 mM, which was approximately 2-fold more potent than chloromycin (MIC = 0.050 mM) and equivalent to norfloxacin (MIC = 0.025 mM). However, when the chlorine atom was replaced by an electron-withdrawing fluorine or electron-donating methoxy group, the biological activity of the resulted 4-fluorophenyl derivative **15a** and 4-methoxyphenyl derivative **15c** decreased, indicating that the electronic effect on the biological activity of the compound is limited. The replacement of 4-fluorophenyl moiety or 4-chlorophenyl group by 2,4-dichlorophenyl and 2,4-difluorophenyl groups, respectively, afforded corresponding *O*-methyl oxime derivatives **15d** and **15e** with weaker activities, which indicated that the position of chlorine or fluorine

atom on phenyl ring played a crucial role for biological activity and the mono-substituted fluorobenzene or chlorobenzene was more beneficial to antimicrobial activity in contrast with difluorophenyl or dichlorophenyl derivatives.

Previous research work including our and other groups has shown that the substitution at the C-6 position of quinolone skeleton also had a significant effect on biological activity [18]. As shown in Table 1, both of the 6-substituted hydroxyl oxime **22a** and *O*-methyl oxime **22b** showed good biological activity. The hydroxyl oxime derivative **22a** could significantly inhibit the growth of *S. aureus* 25923 and *E. coli* with relatively lower MIC values of 0.017 and 0.069 mM, respectively, while *O*-methyl oxime derivative **22b** could effectively inhibit the growth of MRSA and *S. aureus* with the same concentrations of 0.067 mM. However, among the phenyl *O*-methyl oxime fragments incorporated derivatives **23a-d**, except that the 4-fluorophenyl oxime derivative **23a** exhibited good biological activity with the MIC values ranging from 0.014 to 0.461 mM against the tested strains, all the other compounds significantly lose the biological activity or showed even no activity compared to the corresponding 7-substituted counterparts. These results indicated that the introduction of the oxime fragments played an essential role in the antibacterial activity, and it was more effective to be connected at the C-7 position of quinolone.

2.2.2. Antifungal activity

The antifungal evaluation was also carried out and the results revealed that some target oxime derivatives exhibited good potency against the tested fungi. As depicted in Table S1, *O*-methyl oxime derivative **10b** displayed the best antifungal activity, which not only could completely inhibit the growth of *C. albicans* ATCC 90023 with MIC value of 0.017 mM, but also exerted much stronger inhibitory activity against *A. fumigatus* (MIC = 0.035 mM) than fluconazole (MIC = 0.836 mM). It was worthy to note that oxime derivative **10a** exhibited equivalent inhibitions against *C. parapsilosis* ATCC 22019, *C. albicans* as well as *C. albicans* ATCC 90023 with same MIC value of 0.072 mM. Furthermore, *O*-ethyl oxime derivative **10d** showed MIC value of 0.263 mM against *A. fumigatus*, which was 3-fold more active than reference drug fluconazole. In addition, it was found that the hydroxylamine fragment incorporated quinolone derivative **22a** possessed considerable potentiality with MIC values ranging from 0.069 to 0.278 mM. Noticeably, in series of halobenzyl *O*-methyl oxime derivatives, compounds **15b, 15e** and **23a** all exhibited moderate to good antifungal activity against the tested fungi. Especially, derivative **23a** bearing 4-fluorobenzyl fragment showed relatively lower MIC value (0.029 mM) against *A. fumigatus* than fluconazole. These results manifested that this kind of oxime derivatives should have great potentiality for the further development as new antifungal drugs.

*2.3. Combination use effects of the O-methyl oxime derivative **10b** with reference drugs. (MIC = μg/mL)*

Combination therapy is a widely used method for treating various infectious diseases caused by pathogenic bacteria, which can effectively overcome drug resistance and enhance antimicrobial activity [21]. Herein,

drug combination studies of active compound **10b** with clinical antibacterial cefixime and antifungal fluconazole against microorganism were performed, and the combination effects were determined by the calculated fraction inhibitory concentration (FIC) index [22]. The results showed in Table 2 indicated that the treated strains with combined drugs were more susceptible than their individual use, and their combined effects mainly exhibited synergistic and additive effects. Particularly, the combination of compound **10b** with cefixime resulted in excellent antibacterial activity against *S. aureus* with low MIC value of 8.72 μM, which was 4-fold than itself alone. Moreover, compound **10b** also exhibited a significantly improved antibacterial efficacy against drug-resistant MRSA and *K. pneumonia* when it was combined with cefixime. It was worth noting that the combination of compound 1**0b** with clinical antifungal fluconazole also gave good results against all the tested fungi, while *C. tropicals* exhibited additive sensitivity in this combination use. These results revealed that the combination uses of compound **10b** with cefixime or fluconazole could effectively enhance antimicrobial activity, overcome drug resistance and broaden antimicrobial spectrum.

Table 2

2.4. The propensity to induce bacterial resistance

The development of microbial resistance has posed great challenge to human health, and therefore the assessment of resistance to promising drug candidates comes to be a critical criteria in the drug discovery process [23]. Herein, the probability of the highly active compound **10b** to elicit resistance in bacteria was performed against MRSA strain with the clinical antibacterial norfloxacin as a positive control. The results shown in Fig. 3 demonstrated that there was no obvious substantial variation in susceptibility of MRSA to compound **10b** even after 16 passages, while MIC values of norfloxacin toward MRSA increased around 16-fold after the same time, indicating that it was more difficult for active molecule **10b** to trigger the development of bacterial resistance than reference drug norfloxacin. Furthermore, when compound **10b** was combined with cefixime, no drug resistance was obviously generated (green line), which was consistent with the results of the above-mentioned drug combination, which enhanced the antibacterial potentiality of compound **10b** and overcome the drug resistance.

Fig. 3

2.5. Cytotoxicity assay

Studies have shown that there is a good correlation between extracellular cytotoxicity of chemical substances and animal mortality as well as blood drug concentration in human death [24]. The cytotoxic effects of the highly active compound **10b** toward mammalian cell lines (A549 and BEAS-2B cells) were also investigated *via* MTT assay, and doxorubicin with the concentration of 0.50 μM was used as a positive control. As shown in Fig. 4, after treatment with different concentrations of **10b** for 24 hours, the viability

of both cell lines remained above 75% even at the concentrations up to 139.52 μM, suggesting that this molecule possessed less toxicity toward mammalian cell lines.

Fig. 4

2.6. Cell integrity disruption of MRSA induced by active molecule.

To further investigate the possible antibacterial mechanism of this kind of compounds, the ability of compound **10b** to perturb the bacterial cell membrane was studied [25]. The fluorescent nucleic acid dye propidium iodide (PI) was employed to stain the DNA of bacteria, because it could successfully penetrate the cells with compromised or damaged membranes and emit fluorescence upon binding to the DNA [26]. As shown in Fig. 5, there was almost no change in fluorescence intensity in untreated bacteria, while the fluorescence intensity of experimental group increased sharply after the addition of the compound **10b** and it became steady after 100 min. The observed results demonstrated that this molecule had great potentiality to permeabilize the cell membrane by interfering with the integrity of the membrane.

Fig. 5

2.7. Molecular docking study

Bacterial topoisomerase IV and DNA gyrase have been known as prominent targets for quinolone classes of antibiotics, which could control the topological state of DNA during the processes of transcription, replication and recombination [27]. Considering the membrane activity results obtained above, we deduced that the highly active compound **10b** might attack and cause damage to bacterial cell membrane and then entered the cells to further disrupt the functions of topoisomerase IV or DNA gyrase in the cytoplasm, which would in turn lead to cell death. Therefore, a flexible ligand-receptor docking investigation was carried out with topoisomerase IV–DNA complex and gyrase–DNA complex (PDB code: 2XKK and 4DUH, respectively) as representative targets to rationalize the action mechanism of compound **10b** [28]. Docking results (Fig. 6) showed that there was a hydrogen bond between the oxygen atom of *O*-methyl oxime fragment and DA-20 residue with a distance of 1.8 Å. The NH_2 group at the 2-position of thiazole ring could interact with the ASP-1083 residue through hydrogen bond with the distance of 2.1 Å (Fig. 6A). In addition, the alkyl interaction can also be found between the piperazine ring and ARG-418 residue, which further revealed that the introduction of piperazine ring was beneficial. Furthermore, the aromatic ring of quinolone could interact with base DT-15 of DNA *via* π-π stacking (Fig. 6B). The docking model with DNA gyrase indicated that the nitrogen atom on the aminothiazole ring and the oxygen atom of the quinolone ring can form multiple hydrogen bonds with the Arg 136 residue, which might be beneficial for the stability of the **10b**-gyrase–DNA complex (Fig. S2). Furthermore, the nitrogen atom of *O*-methyl oxime fragment also took part in the non-covalent coordination with Asn-46 residue by a hydrogen bond, which further revealed that nitrogen atom played a crucial role in drug molecules. The docking evaluation gave the lowest binding energy of -7.93 kcal/mol between compound **10b** and topoisomerase IV. All these

non-covalent interactions indicated that compound **10b** could disturb the synthesis of bacterial DNA through binding to DNA gyrase or topoisomerase IV to exert good antibacterial activity.

Fig. 6

2.8. Electronic properties

It is well known that the frontier molecular orbitals (FMO), namely the highest occupied molecular orbital (HOMO) and the lowest unoccupied molecular orbital (LUMO), play an extremely important role in the ligand–receptor interactions process because of the reason that the HOMOs and LUMOs are related to the potential and ability of molecules to donate or accept electrons. The concept is usually extended into drug-receptor binding systems to study the pharmacokinetic properties of drugs [29]. As shown in Table 3, The HOMOs of *O*-methyl oxime derivatives **10b**, **15b** and **23a** were primarily concentrated on the quinolone skeleton and the 2-aminothiazole fragment, indicating that these positions might be active sites and biological interactions may occur between these sites and positively charged molecules. Besides, it was worth noting that LUMOs were also mainly localized on the quinolone ring, manifesting that the quinolone ring could not only interact with the electron donor, but also facilitate nucleophilic attacks. However, the substituted oxime fragments and piperazine ring did not directly contribute to any HOMOs and LUMOs, suggesting that these groups might mainly play roles in regulating the physicochemical properties of the molecules. Furthermore, it was found that compound **10b** shown best antibacterial activity possessed the highest energy gap value (ΔE) of 4.024 eV, which made it more reactivity and less stability.

Table 3

Molecular electrostatic potential (MEP) surface can usually effectively indicate the distribution of electron density on the molecular surface, where the positive isosurfaces (blue) represent the electron deficit regions and the negative isosurfaces (red) signify the electron rich regions, which might be responsible for the formation of hydrogen bond and interaction between these sites and biological targets in biological systems. As shown in Figure 7, the positive charge regions (in blue) mainly located on the amino group of thiazole ring (NH_2) and the electronegative area (in red) primarily concentrated on the oxygen atom of the quinolone ring, which was a good explanation why it was easier for amino and oxygen to form hydrogen bonds with topoisomerase IV and DNA gyrase (Fig. 7 and Fig. S2), which was excellent agreement with docking study.

Fig. 7

*2.9. Biosupramolecular interactions between highly active molecule **10b** and DNA*

Deoxyribonucleic acid (DNA), a significant informative molecule with the function of encoding genetic instructions, has been considered as a validated drug target for the extensive exploration of newly

promising DNA-targeting antimicrobial drugs [30]. Due to the medical importance, low cost and ready availability properties of calf thymus DNA, it was always selected as the DNA model to explore the preliminary antibacterial action mechanism of active candidate molecules [31]. Herein, the *in vitro* binding behavior of the active compound **10b** with calf thymus DNA was performed at a molecular level using NR (neutral red dye) as a spectral probe through UV-vis spectroscopy.

*2.9.1. Absorption spectra of DNA in the presence of compound **10b***

The UV-vis absorption spectrum of the molecule is a commonly useful spectral analysis method based on the absorption spectrum generated by intramolecular electronic transitions, and it is widely used in DNA binding studies [32]. The hyperchromaticity and hypochromaticity as important spectral features are usually emplyed to identify the changes of DNA double helix structure, which are generally resulted from the strong interaction of electronic states between an aromatic chromophore and the base pairs of DNA [33]. As shown in Fig. 8, the UV-vis spectra showed that the absorption peak of DNA at 260 nm gave a proportional increase and slight red shift with the sequentially and proportionately increasing amount of compound **10b** under a fixed concentration of DNA. Furthermore, it was observed (inset of Fig. 8) that the measured value of the **10b**–DNA complex was a little higher than the absorption value of the simply sum of free DNA and free compound **10b**, which illustrated that a weak hyperchromic effect existed between DNA and molecule **10b**. This hyperchromic effect and the red shift phenomenon might be the consequence of electrostatic interaction between **10b** and the DNA base, which provided the convincing evidences for the constructional change of DNA duplex and the formation of binary complexes.

$$\frac{A^0}{A-A^0}=\frac{\xi_C}{\xi_{D-C}-\xi_C}+\frac{\xi_C}{\xi_{D-C}-\xi_C}\times\frac{1}{K[\mathrm{Q}]} \qquad (1)$$

On the basis of the variations in these spectra, the binding constant K could be calculated by using equation (1) [34], yielding K = 2.51 × 10^4 L/mol, R = 0.995, SD = 0.077 (R and SD stand for the correlation coefficient and standard deviation, respectively). The plot of $A^0/(A–A^0)$ versus 1/[compound **10b**] was constructed and showed in Fig. S3.

Fig. 8

*2.9.2. The competitive interaction of active molecule **10b** and NR with DNA*

Neutral red (NR) bearing a similar structure to other planar dyes like acridine, thiazine and xanthene has the advantages of lower toxicity, higher stability and more convenient application as compared to other common probes, and it has been proved to bind with DNA by the way of intercalation [35]. Therefore, NR was selected as a spectral probe to study the binding mode of compound **10b** with DNA in the present work, and the absorption spectrum of competitive binding between NR and **10b** with DNA was shown in Fig. 9. It was found that there was an obvious decrease of the absorption spectra around 530 nm along with the increasing concentration of **10b**, which was a reverse process as compared with the absorption of free

NR at the same wavelength [31]. In addition, a gradually increasing absorption at around 276 nm was also observed in the spectra. These apparent spectral changes suggested that **10b** could effectively intercalate into the double helix of DNA by substituting NR in the DNA–NR complex, which might block bacterial DNA replication to exert powerful antibacterial activity.

Fig. 9

*2.10. Supramolecular transportation of the highly active molecule **10b** by human serum albumin (HSA)*

To understand the pharmacological and pharmacodynamic behavior of drugs, the interaction between drugs and HAS was done using Fluorescence quenching mechanism [36]. As shown in Fig. 10, it could be found that HSA had a strong fluorescence emission peak at around 343 nm (red line), whereas in the same wavelength range, compound **10b** only showed a weak fluorescence intensity (blue line), which could be almost ignored. In addition, under the fixed HSA concentration, the intensity of maximum emission peak gave a gradual decrease with the increasing concentrations of **10b,** but the maximum emission wavelength of HSA remained unchanged (black lines), indicating that Trp-214 did not undergo any polarity change, which further suggested that **10b** might interact with HSA through hydrophobic regions located in the HSA. And the fluorescence quenching behavior disclosed that the supramolecular interaction between compound **10b** and human serum albumin (HSA) was a static quenching rather than dynamic quenching, and the binding process was spontaneous, where hydrogen bonds and Van der Waals force played vital roles in the supramolecular transportation of the active compound **10b** by HSA through forming a stable 1:1 supramolecular complex (Supporting Information).

Fig. 10

3. Conclusion

This work explored a class of novel hybrids of quinolone, aminothiazole, piperazine and oxime fragments as potentially multi-targeting antimicrobial agents for the first time. A series of piperazine-bridged aminothiazolquinolone oximes have been successfully developed, and tested for their *in vitro* antimicrobial activities. Some of the synthesized compounds exhibited moderate to good antimicrobial activities. SAR study revealed that the positions of the oxime fragments at the quinolone skeleton exerted a significant impact on biological activity. Especially, C-7 substituted *O*-methyl oxime derivative **10b** displayed excellent inhibitory efficacy against MRSA and *S. aureus* 25923 with MIC values of 0.009 and 0.017 mM, respectively. Further experiments indicated that this molecule showed low toxicity against A549 and BEAS-2B cell lines and no obvious propensity to trigger the development of bacterial resistance. Quantum chemical studies have rationally explained the structural features essential for activity. The preliminarily mechanism exploration revealed that compound **10b** could effectively permeate bacterial membrane, interact with topoisomerase IV through hydrogen bonds and π-π stacking, and intercalate into DNA to form a stable supramolecular complex, which might be responsible for the powerful bioactivity.

Furthermore, the active molecule **10b** could be effectively transported by HSA *via* hydrogen bonds and Van der Waals force, and the transportation mechanism was static rather than dynamic. These results revealed that *O*-methyl oxime derivative **10b** could be served as a promising candidate in the development of potent antimicrobial agents.

4. Experimental

4.1. General methods

All the chemicals, reagents and organic solvents were commercially available and used directly without further purification. The samples were weighed on a microbalance with a resolution of 0.1 mg. Thin-layer chromatography (TLC) analysis were carried out through pre-coated silica gel plates. Column chromatography was performed by silica gel (#100–200). NMR spectra were recorded on Bruker AVANCE III 600 MHz spectrometer using DMSO-d_6 as solvent, or TMS as internal standard. The chemical shifts were reported in parts per million (ppm), the coupling constants (*J*) were expressed in hertz unit (Hz) and signals were described as singlet (s), doublet (d), triplet (t), broad (br) as well as multiplet (m). The high-resolution mass spectra (HRMS) were recorded on IonSpec FT–CR mass spectrometer with ESI resource. Melting point (mp) was measured on a melting point apparatus (X-6 type). All fluorescence spectra were recorded on F-7000 spectrofluorimeter (Hitachi, Tokyo, Japan) and UV spectra were obtained through TU-2450 spectrophotometer (Puxi Analytic Instrument Ltd. of Beijing, China), both of which were equipped with 1.0 cm quartz cells. The microbial strains were provided by Sichuan Provincial People's Hospital (Chengdu, China) and the neutral red (NR) and DNA were purchased from Sigma-Aldrich (St. Louis, MO, USA). Quantitative nuclear magnetic resonance (QNMR) was used to determine the purity of the target compounds using 1,3,5-trioxane as the internal standard. The results indicated that all the target compounds possessed purity ≥ 95%.

*4.1.1. General experimental procedures for the synthesis of the desired intermediates (**2–7**).*

The desired intermediates **2–7** were prepared according to the previously reported methods [18].

*4.1.2. General experimental procedures for the synthesis of the desired intermediates (**13a-e** and **14a-e**)*

The desired intermediates **13a-e** and **14a-e** were prepared according to the previously reported methods [37].

*4.1.3. Synthesis of 3-(2-Aminothiazol-4-yl)-1-ethyl-6-fluoro-7-(piperazin-1-yl)quinolin-4(1H)-one (**8**).*

A mixture of intermediate **7** (4.86 g, 15.00 mmol) and piperazine (3.87 g, 45.00 mmol) in 1-methyl-2-pyrrolidinone (NMP) (20 mL) was stirred at 130 ºC for 24 h. After completion of the reaction, the solvent was evaporated under reduced pressure and the residue was diluted with water (200 mL), and then extracted with chloroform (3 × 100 mL). The combined organic layers were dried over anhydrous sodium sulfate, filtered and concentrated. The crude product was purified *via* silica gel column chromatography (eluent, chloroform/ methanol (V/V) = 15/1) to afford compound **8** (1.19 g) as yellow solid. Yield: 21.3%;

mp: > 250 ºC; ^{1}H NMR (600 MHz, DMSO-d_6) δ 8.59 (s, 1H, quinolone-2-*H*), 7.86 (d, *J* = 13.7 Hz, 1H, quinolone-5-*H*), 7.63 (s, 1H, thiazole-4-*H*), 7.01 (d, *J* = 7.2 Hz, 1H, quinolone-8-*H*), 6.92 (s, 2H, thiazole-2-NH_2), 4.38 (q, *J* = 7.0 Hz, 2H, CH_2CH$_3$), 3.15 (t, *J* = 4.02 Hz, 4H, piperazine-2,2-*N*-(CH_2)$_2$), 2.91 (t, *J* = 4.38 Hz, 4H, piperazine-3,3-*N*-(CH_2)$_2$), 1.38 (t, *J* = 7.1 Hz, 3H, CH$_2$CH_3) ppm; ^{13}C NMR (151 MHz, DMSO-d_6) δ 172.9, 167.1, 151.8, 144.9, 144.7, 142.6, 136.1, 121.5, 114.9, 111.9, 105.3, 103.9, 51.2, 49.1, 48.4, 45.7, 14.8 ppm.

*4.1.4. Synthesis of 3-(2-Aminothiazol-4-yl)-1-ethyl-6-fluoro-7-(4-(2-oxopropyl)piperazin-1-yl)quinolin-4(1H)-one (**9**).*

A mixture of intermediate **8** (186.73 mg, 0.50 mmol) and potassium carbonate (103.66 mg, 0.75 mmol) in acetonitrile (25 mL) was stirred at 60 ºC for 1.5 h, and then cooled to room temperature. To the reaction system was added slowly 1-Chloropropan-2-one (69.39 mg, 0.75 mmol), and the resulting mixture was stirred at 80 ºC for 6 h. After the completion of reaction, the solvent was evaporated under reduced pressure and the residue was diluted with water (100 mL), and then extracted with chloroform (3 × 50 mL). The organic extracts were dried over anhydrous sodium sulfate and concentrated. The crude product was purified by silicagel column chromatography (eluent, chloroform/methanol (V/V) = 25/1) to afford target compound **9** (143.24 mg) as yellow solid. Yield: 66.7%; mp: 163–165 ºC; ^{1}H NMR (600 MHz, DMSO-d_6) δ 8.59 (s, 1H, quinolone-2-*H*), 7.86 (d, *J* = 13.6 Hz, 1H, quinolone-5-*H*), 7.63 (s, 1H, thiazole-4-*H*), 7.05 (d, *J* = 7.3 Hz, 1H, quinolone-8-*H*), 6.90 (s, 2H, thiazole-2-NH_2), 4.38 (q, *J* = 7.1 Hz, 2H, CH_2CH$_3$), 3.28 (s, 2H, CH_2COCH$_3$), 3.27–3.22 (m, 4H, piperazine-2,2-*N*-(CH_2)$_2$), 2.66–2.60 (m, 4H, piperazine-3,3-*N*-(CH_2)$_2$), 2.11 (s, 3H, CH$_2$COCH_3), 1.39 (t, *J* = 7.2 Hz, 3H, CH$_2$CH_3) ppm; ^{13}C NMR (151 MHz, DMSO-d_6) δ 207.1, 172.9, 167.1, 151.7, 144.9, 144.2, 142.7, 136.1, 121.6, 114.9, 111.8, 105.5, 103.9, 67.7, 52.9, 50.2, 49.1, 48.4, 28.1, 14.8 ppm; HRMS (ESI) calcd. for $C_{21}H_{24}FN_5O_2S$ $[M + H]^+$, 430.1713; found, 430.1710.

*4.1.5. Synthesis of (E)-3-(2-Aminothiazol-4-yl)-1-ethyl-6-fluoro-7-(4-(2-(hydroxyimino)propyl)piperazin-1-yl)quinolin-4(1H)-one (**10a**).*

A mixture of intermediate **9** (214.75 mg, 0.50 mmol), potassium carbonate (103.66 mg, 0.75 mmol) and hydroxylamine hydrochloride (52.11 mg, 0.75 mmol) in acetonitrile (25 mL) was stirred at 80 ºC for 6 h. After the completion of reaction, the solvent was evaporated under reduced pressure and the residue was diluted with water (100 mL), and then extracted with chloroform (3 × 50 mL). The organic extracts were dried over anhydrous sodium sulfate and concentrated. The crude product was purified *via* silica gel column chromatography (eluent, chloroform/methanol (V/V) = 25/1) to afford target compound **10a** (149.58 mg) as light yellow solid. Yield: 67.3%; mp: > 250 ºC; ^{1}H NMR (600 MHz, DMSO-d_6) δ 10.58 (s, 1H, O*H*), 8.59 (s, 1H, quinolone-2-*H*), 7.86 (d, *J* = 13.6 Hz, 1H, quinolone-5-*H*), 7.63 (s, 1H, thiazole-4-*H*), 7.05 (d, *J* = 7.1 Hz, 1H, quinolone-8-*H*), 6.92 (s, 2H, thiazole-2-NH_2), 4.38 (dd, *J* = 13.8, 6.7 Hz, 2H, CH_2CH$_3$), 3.24 (s, 4H, piperazine-2,2-*N*-(CH_2)$_2$), 3.04 (s, 2H, CH_2C(N-OH)CH$_3$), 2.54 (s, 4H,

piperazine-3,3-*N*-(CH_2)$_2$), 1.81 (s, 3H, CH_3), 1.38 (t, *J* = 7.1 Hz, 3H, CH$_2$CH_3) ppm; ^{13}C NMR (151 MHz, DMSO-d_6) δ 172.9, 167.1, 153.4, 144.9, 144.2, 142.7, 136.1, 121.6, 114.9, 111.7, 105.6, 103.9, 62.1, 52.9, 50.2, 48.4, 14.8, 12.7 ppm; HRMS (ESI) calcd. for $C_{21}H_{26}FN_6O_2S$ [M + H]$^+$, 445.1822; found, 445.1815.

*4.1.6. Synthesis of (E)-3-(2-Aminothiazol-4-yl)-1-ethyl-6-fluoro-7-(4-(2-(methoxyimino)propyl)piperazin -1-yl)quinolin-4(1H)-one (**10b**).*

Compound **10b** was prepared according to the experimental procedure described for compound **10a** starting from intermediate **9** (214.75 mg, 0.50 mmol), potassium carbonate (103.66 mg, 0.75 mmol) and *O*-methylhydroxylamine hydrochloride (41.76 mg, 0.50 mmol). The target compound **10b** (141.11 mg) was obtained as light yellow solid. Yield: 61.6%; mp: 230–232 ºC; ^{1}H NMR (600 MHz, DMSO-d_6) δ 8.59 (s, 1H, quinolone-2-*H*), 7.86 (d, *J* = 13.6 Hz, 1H, quinolone-5-*H*), 7.63 (s, 1H, thiazole-4-*H*), 7.05 (d, *J* = 7.1 Hz, 1H, quinolone-8-*H*), 6.92 (s, 2H, thiazole-2-NH_2), 4.38 (dd, *J* = 13.9, 6.9 Hz, 2H, CH_2CH$_3$), 3.78 (s, 3H, OCH_3), 3.24 (s, 4H, piperazine-2,2-*N*-(CH_2)$_2$), 3.03 (s, 2H, CH_2C(N-OCH$_3$)CH$_3$), 2.55 (s, 4H, piperazine-3,3-*N*-(CH_2)$_2$), 1.84 (s, 3H, CH_3), 1.38 (t, *J* = 7.1 Hz, 3H, CH$_2$CH_3) ppm; ^{13}C NMR (151 MHz, DMSO-d_6) δ 172.9, 167.1, 155.4, 153.4, 144.9, 144.2, 142.6, 136.1, 121.6, 114.9, 111.7, 105.5, 103.9, 61.6, 61.4, 52.9, 50.2, 49.7, 48.4, 14.8, 13.3 ppm; HRMS (ESI) calcd. for $C_{22}H_{27}FN_6O_2S$ [M + H]$^+$, 459.1978; found, 459.1974.

*4.1.7. Synthesis of (E)-3-(2-Aminothiazol-4-yl)-1-ethyl-6-fluoro-7-(4-(2-(methoxyimino)propyl)piperazin -1-yl)quinolin-4(1H)-one (**10c**).*

Compound **10c** was prepared according to the experimental procedure described for compound **10a** starting from intermediate **9** (214.75 mg, 0.50 mmol), potassium carbonate (103.66 mg, 0.75 mmol) and *O*-ethylhydroxylamine hydrochloride (73.16 mg, 0.75 mmol). The target compound **10c** (133.40 mg) was obtained as yellow solid. Yield: 56.5%; mp: 202–204 ºC; ^{1}H NMR (600 MHz, DMSO-d_6) δ 8.59 (s, 1H, quinolone-2-*H*), 7.86 (d, *J* = 13.6 Hz, 1H, quinolone-5-*H*), 7.63 (s, 1H, thiazole-4-*H*), 7.04 (d, *J* = 7.2 Hz, 1H, quinolone-8-*H*), 6.91 (s, 2H, thiazole-2-NH_2), 4.38 (q, *J* = 7.1 Hz, 2H, CH_2CH$_3$), 4.04 (q, *J* = 7.0 Hz, 2H, OCH_2CH$_3$), 3.24 (s, 4H, piperazine-2,2-*N*-(CH_2)$_2$), 3.04 (s, 2H, CH_2C(*N*-OCH$_2$CH$_3$)CH$_3$), 2.55 (s, 4H, piperazine-3,3-*N* -(CH_2)$_2$), 1.85 (s, 3H, CH_3), 1.39 (t, *J* = 7.2 Hz, 3H, *N*-CH$_2$CH_3), 1.19 (t, *J* = 7.0 Hz, 3H, OCH$_2$CH_3) ppm; ^{13}C NMR (151 MHz, DMSO-d_6) δ 172.9, 167.1, 154.9, 153.4, 151.8, 144.9, 142.7, 136.1, 121.6, 114.9, 111.9, 105.6, 103.9, 68.7, 61.8, 52.9, 50.2, 48.4, 15.1, 14.8, 13.4 ppm; HRMS (ESI) calcd. for $C_{23}H_{29}FN_6O_2S$ [M + H]$^+$, 473.2135; found, 473.2133.

*4.1.8. Synthesis of (E)-2-(1-(4-(3-(2-Aminothiazol-4-yl)-1-ethyl-6-fluoro-4-oxo-1,4-dihydroquinolin-7 -yl)piperazin-1-yl)propan-2-ylidene)hydrazine-1-carboxamide (**10d**).*

Compound **10d** was prepared according to the experimental procedure described for compound **10a** starting from intermediate **9** (214.75 mg, 0.50 mmol), potassium carbonate (103.66 mg, 0.75 mmol) and aminourea hydrochloride (83.65 mg, 0.75 mmol). The target compound **10d** (127.87 mg) was obtained as white solid. Yield: 52.6%; mp: > 250 ºC; ^{1}H NMR (600 MHz, DMSO-d_6) δ 9.06 (s, 1H, N-N*H*CONH$_2$),

8.59 (s, 1H, quinolone-2-*H*), 7.86 (d, *J* = 13.6 Hz, 1H, quinolone-5-*H*), 7.64 (s, 1H, thiazole-4-*H*), 7.04 (d, *J* = 7.2 Hz, 1H, quinolone-8-*H*), 6.91 (s, 2H, thiazole-2-NH_2), 6.24 (s, 2H, N-NHCONH_2), 4.38 (q, *J* = 7.0 Hz, 2H, CH_2CH$_3$), 3.24 (s, 4H, piperazine-2,2-*N*-(CH_2)$_2$), 3.07 (s, 2H, CH_2C(*N*- NHCONH$_2$)CH$_3$), 2.55 (s, 4H, piperazine-3,3-*N*-(CH_2)$_2$), 1.87 (s, 3H, CH_3), 1.39 (t, *J* = 7.1 Hz, 3H, CH$_2$CH_3) ppm; ^{13}C NMR (151 MHz, DMSO-d_6) δ 172.9, 167.1, 157.6, 153.4, 151.8, 144.9, 142.7, 136.1, 121.6, 114.9, 111.7, 105.5, 103.9, 64.9, 52.9, 50.3, 48.4, 14.9, 14.7 ppm; HRMS (ESI) calcd. for $C_{22}H_{27}FN_8O_2S$ $[M + H]^+$, 487.2040; found, 487.2036.

*4.1.9. Synthesis of (E)-3-(2-Aminothiazol-4-yl)-1-ethyl-6-fluoro-7-(4-(2-(methoxyimino)propyl)piperazin -1-yl)quinolin-4(1H)-one (**11**).*

A mixture of compound **10a** (222.09 mg, 0.50 mmol) and potassium carbonate (103.66 mg, 0.75 mmol) in acetonitrile (25 mL) was stirred at 60 ºC for 1.5 h, and then cooled to room temperature. To the reaction system was added 2,4-Dichlorobenzyl chloride (293.21 mg, 1.50 mmol), and the resulting mixture was stirred at 80 ºC for 12 h. After the completion of reaction, the solvent was evaporated under reduced pressure and the residue was diluted with water (50 mL), and then extracted with chloroform (3 × 20 mL). The organic extracts were dried over anhydrous sodium sulfate and concentrated. The crude product was purified *via* silicagel column chromatography (eluent, dichloromethane/methanol (V/V) = 50/2) to afford target compound **11** (153.25 mg) as yellow solid. Yield: 50.9%; mp: > 250 ºC; ^{1}H NMR (600 MHz, DMSO-d_6) δ 8.60 (s, 1H, quinolone-2-*H*), 7.87 (d, *J* = 13.6 Hz, 1H, quinolone-5-*H*), 7.64 (s, 1H, thiazole-4-*H*), 7.62 (s, 1H, 2,4-diCl-Ph-3-*H*), 7.45 (s, 2H, 2,4-diCl-Ph-4,5-2*H*), 7.04 (d, *J* = 7.2 Hz, 1H, quinolone-8-*H*), 6.94 (s, 2H, thiazole-2-NH_2), 5.14 (s, 2H, 2,4-2ClPh-CH_2), 4.38 (q, *J* = 7.0 Hz, 2H, CH_2CH$_3$), 3.24 (s, 4H, piperazine-2,2-*N*-(CH_2)$_2$), 3.07 (s, 2H, CH_2C(N-OCH$_2$- 2,4-2Cl-Ph)CH$_3$), 2.54 (s, 4H, piperazine-3,3-*N*-(CH_2)$_2$), 1.93 (s, 3H, -CH_3), 1.39 (t, *J* = 7.1 Hz, 3H, CH$_2$CH_3) ppm; ^{13}C NMR (151 MHz, DMSO-d_6) δ 172.9, 167.1, 153.4, 144.8, 142.7, 136.1, 135.2, 133.7, 133.5, 132.2, 131.9, 131.7, 129.1, 127.7, 121.6, 114.8, 111.9, 105.5, 103.9, 71.9, 67.9, 52.8, 50.1, 48.4, 14.8, 14.3 ppm; HRMS (ESI) calcd. for $C_{28}H_{29}Cl_2FN_6O_2S$ $[M + H]^+$, 603.1512; found, 603.1486.

*4.1.10. Synthesis of (E)-3-(2-Aminothiazol-4-yl)-1-ethyl-6-fluoro-7-(4-(2-(4-fluorophenyl)-2-(methoxyimino)ethyl)piperazin-1-yl)quinolin- 4(1H)-one (**15a**).*

A mixture of compound **8** (186.57 mg, 0.50 mmol) and potassium carbonate (103.66 mg, 0.75 mmol) in acetonitrile (25 mL) was stirred at 60 ºC for 1.5 h, and then cooled to room temperature. Intermediate **14a** (150.78 mg, 0.75 mmol) was added, and the resulting mixture was stirred at 80 ºC for 10 h. After the completion of reaction, the solvent was evaporated under reduced pressure and the residue was diluted with water (50 mL), and then extracted with chloroform (3 × 20 mL). The organic extracts were dried over anhydrous sodium sulfate and concentrated. The crude product was purified *via* silica gel column chromatography (eluent, dichloromethane/methanol (V/V) = 50/2) to afford target compound **15a** (171.68 mg) as yellow solid. Yield: 63.8%; mp: 230–232 ºC; ^{1}H NMR (600 MHz, DMSO-d_6) δ 8.58 (s, 1H,

quinolone-2-*H*), 7.86 (d, *J* = 7.3 Hz, 1H, quinolone-5-*H*), 7.84 (d, *J* = 2.8 Hz, 1H, 4-F-Ph-2-*H*), 7.83 (d, *J* = 2.0 Hz, 1H, 4-F-Ph-6-*H*), 7.64 (s, 1H, thiazole-4-*H*), 7.23 (t, *J* = 8.9 Hz, 2H, 4-F-Ph-3,5-2*H*), 7.01 (d, *J* = 7.2 Hz, 1H, quinolone-8-*H*), 6.93 (s, 2H, thiazole-2-NH_2), 4.36 (q, *J* = 7.1 Hz, 2H, CH_2CH$_3$), 3.94 (s, 3H, OCH_3), 3.72 (s, 2H, CH_2C(N-OCH$_3$)), 3.15 (s, 4H, piperazine-2,2-*N*-(CH_2)$_2$), 2.62 (s, 4H, piperazine-3,3-*N*-(CH_2)$_2$), 1.36 (d, *J* = 7.0 Hz, 3H, CH$_2$CH_3) ppm; ^{13}C NMR (151 MHz, DMSO-d_6) δ 172.9, 167.4, 167.1, 163.9, 162.3, 153.9, 151.8, 144.8, 144.2, 142.7, 136.0, 132.2, 132.0, 129.4, 129.1, 121.7, 115.6, 115.4, 114.8, 111.8, 105.6, 103.9, 62.3, 53.2, 51.2, 50.2, 49.1, 48.4, 14.8 ppm; HRMS (ESI) calcd. for $C_{27}H_{28}F_2N_6O_2S$ $[M + H]^+$, 539.2041; found, 539.2040.

*4.1.11. Synthesis of (E)-3-(2-Aminothiazol-4-yl)-7-(4-(2-(4-chlorophenyl)-2-(methoxyimino)ethyl) piperazin-1-yl)-1-ethyl-6-fluoroquinolin -4(1H)-one (**15b**).*

Compound **15b** was prepared according to the experimental procedure described for compound **15a** starting from intermediate **14b** (162.75 mg, 0.75 mmol), potassium carbonate (103.66 mg, 0.75 mmol) and compound **8** (186.73 mg, 0.50 mmol). The target compound **15b** (174.84 mg) was obtained as light yellow solid. Yield: 63.1%; mp: 220–222 ºC; ^{1}H NMR (600 MHz, DMSO-d_6) δ 8.57 (s, 1H, quinolone-2-*H*), 7.85 (d, *J* = 13.6 Hz, 1H, quinolone-5-*H*), 7.81 (s, 1H, 4-Cl-Ph-2-*H*), 7.80 (s, 1H, 4-Cl-Ph-6-*H*), 7.63 (s, 1H, thiazole-4-*H*), 7.46 (s, 1H, 4-Cl-Ph-3-*H*), 7.45 (s, 1H, 4-Cl-Ph-5-*H*), 7.00 (d, *J* = 7.2 Hz, 1H, quinolone-8-*H*), 6.86 (s, 2H, thiazole-2-NH_2), 4.34 (q, *J* = 7.1 Hz, 2H, CH_2CH$_3$), 3.94 (s, 3H, OCH_3), 3.72 (s, 2H, CH_2C(N-OCH$_3$), 3.15 (s, 4H, piperazine-2,2-*N*-(CH_2)$_2$), 2.61 (s, 4H, piperazine-3,3-*N*-(CH_2)$_2$), 1.36 (t, *J* = 7.1 Hz, 3H, 3H, CH$_2$CH_3) ppm; ^{13}C NMR (151 MHz, DMSO-d_6) δ 172.9, 167.1, 153.9, 153.4, 151.8, 144.9, 144.2, 142.7, 136.0, 134.3, 128.9, 128.6, 121.6, 114.9, 111.8, 111.7, 105.6, 103.9, 62.4, 53.0, 51.1, 50.2, 49.1, 48.4, 14.8 ppm; HRMS (ESI) calcd. for $C_{27}H_{28}ClFN_6O_2S$ $[M + H]^+$, 555.1745; found, 555.1740.

*4.1.12. Synthesis of (E)-3-(2-Aminothiazol-4-yl)-1-ethyl-6-fluoro-7-(4-(2-(methoxyimino)-2-(4-methoxyphenyl)ethyl)piperazin-1-yl)quinolin -4(1H)-one (**15c**).*

Compound **15c** was prepared according to the experimental procedure described for compound **15a** starting from intermediate **14c** (159.79 mg, 0.75 mmol), potassium carbonate (103.66 mg, 0.75 mmol) and compound **8** (186.73 mg, 0.50 mmol). The target compound **15c** (162.59 mg) was obtained as yellow solid. Yield: 59.1%; mp: 197–199 ºC; ^{1}H NMR (600 MHz, DMSO-d_6) δ 8.57 (s, 1H, quinolone-2-*H*), 7.85 (d, *J* = 13.6 Hz, 1H, quinolone-5-*H*), 7.74 (d, *J* = 2.0 Hz, 1H, 4-CH$_3$O-Ph-2-*H*), 7.73 (s, 1H, 4-CH$_3$O-Ph-6-*H*), 7.63 (s, 1H, thiazole-4-*H*), 7.01 (d, *J* = 7.2 Hz, 1H, quinolone-8-*H*), 6.95 (s, 1H, 4-CH$_3$O-Ph-3-*H*), 6.94 (s, 1H, 4-CH$_3$O-Ph-5-*H*), 6.91 (s, 2H, thiazole-2-NH_2), 4.35 (q, *J* = 7.1 Hz, 2H, CH_2CH$_3$), 3.91 (s, 3H, -OCH_3), 3.78 (s, 3H, Ph-OCH_3), 3.69 (s, 2H, CH_2C(N-OCH$_3$), 3.15 (s, 4H, piperazine-2,2-*N*-(CH_2)$_2$), 2.62 (s, 4H, piperazine-3,3-*N*-(CH_2)$_2$), 1.35 (t, *J* = 7.1 Hz, 3H, CH$_2$CH_3) ppm; ^{13}C NMR (151 MHz, DMSO-d_6) δ 172.9, 167.1, 160.5, 154.2, 153.4, 151.8, 144.9, 144.2, 142.7, 136.0, 128.5, 121.6, 114.9, 114.0, 111.8,

111.7, 105.6, 103.9, 62.1, 55.7, 53.1, 51.1, 50.3, 48.4, 14.8 ppm; HRMS (ESI) calcd. for $C_{28}H_{31}FN_6O_3S$ [M + H]$^+$, 551.2241; found, 551.2236.

*4.1.13. Synthesis of (E)-3-(2-Aminothiazol-4-yl)-7-(4-(2-(2,4-dichlorophenyl)-2-(methoxyimino)ethyl)-piperazin-1-yl)-1-ethyl-6-fluoro quinolin-4(1H)-one (**15d**)*

Compound **15d** was prepared according to the experimental procedure described for compound **15a** starting from intermediate **14d** (188.23 mg, 0.75 mmol), potassium carbonate (103.66 mg, 0.75 mmol) and compound **8** (186.73 mg, 0.50 mmol). The target compound **15d** (177.61 mg) was obtained as yellow solid. Yield: 60.4%; mp: 140–142 ºC; ^{1}H NMR (600 MHz, DMSO-d_6) δ 8.57 (s, 1H, quinolone-2-*H*), 7.83 (d, J = 13.6 Hz, 1H, quinolone-5-*H*), 7.68 (d, J = 2.0 Hz, 1H, 2,4-diCl-Ph-6-*H*), 7.62 (s, 1H, thiazole-4-*H*), 7.50 (s, 1H, 2,4-diCl-Ph-3-*H*), 7.48 (d, J = 2.0 Hz, 1H, 2,4-diCl-Ph-5-*H*), 6.96 (d, J = 7.3 Hz, 1H, quinolone-8-*H*), 6.92 (s, 2H, thiazole-2-NH_2), 4.35 (q, J = 7.1 Hz, 2H, CH_2CH$_3$), 3.91 (s, 3H, -OCH_3), 3.70 (s, 2H, CH_2C(N-OCH$_3$), 3.03 (s, 4H, piperazine-2,2-*N*-(CH_2)$_2$), 2.55 (d, J = 3.9 Hz, 4H, piperazine-3,3-*N*-(CH_2)$_2$), 1.35 (t, J = 7.1 Hz, 3H, CH$_2$CH_3) ppm; ^{13}C NMR (151 MHz, DMSO-d_6) δ 172.9, 167.1, 156.6, 153.3, 151.7, 144.9, 144.1, 142.6, 136.0, 134.3, 133.9, 132.8, 129.3, 127.5, 121.6, 114.9, 111.7, 105.5, 103.9, 62.4, 54.2, 53.4, 50.1, 48.3, 14.9 ppm; HRMS (ESI) calcd. for $C_{27}H_{27}Cl_2FN_6O_2S$ [M + H]$^+$, 589.1356; found, 589.1348.

*4.1.14. Synthesis of (E)-3-(2-Aminothiazol-4-yl)-7-(4-(2-(2,4-difluorophenyl)-2-(methoxyimino)ethyl)-piperazin-1-yl)-1-ethyl-6-fluoro- quinolin-4(1H)-one (**15e**).*

Compound **15e** was prepared according to the experimental procedure described for compound **15a** starting from intermediate **14e** (164.27 mg, 0.75 mmol), potassium carbonate (103.66 mg, 0.75 mmol) and compound **8** (186.73 mg, 0.50 mmol). The target compound **15e** (151.84 mg) was obtained as yellow solid. Yield: 54.6%; mp: 144–146 ºC; ^{1}H NMR (600 MHz, DMSO-d_6) δ 8.57 (s, 1H, quinolone-2-*H*), 7.83 (d, J = 13.6 Hz, 1H, quinolone-5-*H*), 7.69–7.65 (m, 1H, 2,4-diF-Ph-6-*H*), 7.63 (s, 1H, thiazole-4-*H*), 7.31–7.27 (m, 1H, 2,4-diF-Ph-5-*H*), 7.13 (td, J = 8.4, 2.4 Hz, 1H, 2,4-diF-Ph-3-*H*), 6.97 (d, J = 7.3 Hz, 1H, quinolone -8-*H*), 6.91 (s, 2H, thiazole-2-NH_2), 4.35 (d, J = 7.1 Hz, 2H, CH_2CH$_3$), 3.92 (s, 3H, -OCH_3), 3.68 (s, 2H, CH_2C(N-OCH$_3$)), 3.06 (s, 4H, piperazine-2,2-*N*-(CH_2)$_2$), 2.56–2.52 (m, 4H, piperazine-3,3-*N*-(CH_2)$_2$), 1.35 (t, J = 7.2 Hz, 3H, CH$_2$CH_3) ppm; ^{13}C NMR (151 MHz, DMSO-d_6) δ 172.9, 167.1, 162.1, 153.9, 153.3, 151.7, 144.9, 144.1, 142.6, 136.0, 131.9, 129.2, 121.6, 114.9, 111.8, 105.5, 104.6, 103.9, 62.4, 53.5, 53.2, 50.1, 48.3, 14.8 ppm; HRMS (ESI) calcd. for $C_{27}H_{27}F_3N_6O_2S$ [M + H]$^+$, 557.1947; found, 557.1940.

*4.1.15. Synthesis of 3-Acetyl-7-chloro-1-ethyl-6-(piperazin-1-yl)quinolin-4(1H)-one (**16**).*

A mixture of compound **5** (4.00 g, 14.98 mmol), triethylamine (6.06 g, 59.92 mmol), and piperazine (5.16 g, 59.92 mmol) was stirred at 140 ºC in DMSO (30 mL) for 12 h. After completion of the reaction, the solvent was evaporated under reduced pressure and the residue was diluted with water (200 mL), and then extracted with chloroform (3 × 100 mL). The organic extracts were dried over anhydrous sodium sulfate

and concentrated. The crude product was purified *via* silica gel column chromatography (eluent, chloroform/methanol (V/V) = 15/1) to afford compound **16** (1.95 g) as yellow solid. Yield: 39.2%.

*4.1.16. Synthesis of Tert-butyl4-(3-acetyl-7-chloro-1-ethyl-4-oxo-1,4-dihydroquinolin-6-yl)piperazine-1-carboxylate (**17**).*

A mixture of compound **16** (1.50 g, 4.50 mmol), triethylamine (0.91 g, 9.01 mmol), and di-tert-butyl pyrocarbonate (1.96 g, 9.01 mmol) was stirred at room temperature in dichloromethane (100 mL) for 12 h. After completion of the reaction, the solvent was evaporated under reduced pressure and the residue was diluted with water (100 mL), and then extracted with chloroform (3 × 50 mL). The organic extracts were dried over anhydrous sodium sulfate and concentrated. The crude product was purified *via* silica gel column chromatography (eluent, ethyl acetate/ petroleum ether (V/V) = 1/3) to afford compound **17** (1.53 g) as light yellow solid. Yield: 78.6%; mp: 243–245 ºC; ^{1}H NMR (600 MHz, DMSO-d_6) δ 8.60 (s, 1H, quinolone-2-*H*), 8.00 (s, 1H, quinolone-5-*H*), 7.94 (s, 1H, quinolone-8-*H*), 4.43 (q, *J* = 7.1 Hz, 2H, CH_2CH$_3$), 3.52 (s, 4H, piperazine-3,3-*N*-(CH_2)$_2$), 3.03–2.99 (m, 4H, piperazine-2,2-*N*-(CH_2)$_2$), 2.61 (s, 3H, COCH_3), 1.44 (s, 9H, Boc-CH_3), 1.34 (t, *J* = 7.1 Hz, 3H, CH$_2$CH_3) ppm; ^{13}C NMR (151 MHz, DMSO-d_6) δ 196.3, 174.2, 154.4, 148.4, 146.6, 135.4, 134.2, 129.0, 119.7, 118.1, 117.6, 79.6, 51.5, 48.6, 31.6, 28.6, 14.9 ppm; HRMS (ESI) calcd. for $C_{22}H_{28}ClN_3O_4$ [M + H]$^+$, 434.1847; found, 434.1842.

*4.1.17. Synthesis of Tert-butyl 4-(7-chloro-3-(2,2-dibromoacetyl)-1-ethyl-4-oxo -1,4-dihydroquinolin-6-yl)piperazine-1-carboxylate (**18**).*

To a solution of compound **17** (1.00 g, 2.31 mmol) in ethyl acetate (150 mL) was added cupric bromide (1.03 g, 4.62 mmol). The mixture was then stirred at 78 ºC for 12 h. After completion of the reaction, the solvent was evaporated under reduced pressure and the residue was washed with methanol and dichloromethane (200 mL, (V/V) = 2/1). The organic solvents were dried over anhydrous sodium sulfate and concentrated. The crude product was purified *via* silica gel column chromatography (eluent, ethyl acetate/ petroleum ether (V/V) = 1/8) to afford compound **18** (0.83 g) as yellow solid. Yield: 61.2%; mp: > 250 ºC; ^{1}H NMR (600 MHz, CDCl$_3$) δ 8.64 (s, 1H, quinolone-2-*H*), 8.12 (s, 1H, quinolone-5-*H*), 7.88 (s, 1H, quinolone-8-*H*), 7.59 (s, 1H, COC*H*Br$_2$), 4.31 (q, *J* = 7.2 Hz, 2H, CH_2CH$_3$), 3.63 (d, *J* = 4.2 Hz, 4H, piperazine-3,3-*N*-(CH_2)$_2$), 3.11–3.08 (m, 4H, piperazine-2,2-*N*-(CH_2)$_2$), 1.61 (t, *J* = 7.2 Hz, 3H, CH$_2$CH_3), 1.50 (s, 9H，Boc-CH_3) ppm; ^{13}C NMR (151 MHz, CDCl$_3$) δ 185.6, 174.0, 154.8, 149.2, 147.7, 135.5, 134.6, 128.6, 118.6, 118.4, 112.6, 80.1, 51.4, 49.6, 44.6, 28.5, 14.6 ppm; HRMS (ESI) calcd. for $C_{22}H_{26}Br_2ClN_3O_4$ [M + H]$^+$, 590.0057; found, 590.0053.

*4.1.18. Synthesis of Tert-butyl 4-(3-(2-aminothiazol-4-yl)-7-chloro-1-ethyl-4-oxo -1,4-dihydroquinolin-6-yl)piperazine-1-carboxylate (**19**).*

A mixture of intermediate **18** (0.60 g, 1.02 mmol) and thiourea (93.04 mg, 1.22 mmol) was stirred at 80 ºC in ethanol (100 mL) for 4 h. After completion of the reaction, the solvent was evaporated under reduced pressure and the residue was diluted with water (100 mL), and then extracted with chloroform (3 x 50 mL).

The organic extracts were dried over anhydrous sodium sulfate and concentrated. The crude product was purified *via* silica gel column chromatography (eluent, chloroform/methanol (V/V) = 50/1) to afford compound **19** (0.30 g) as yellow solid. Yield: 59.2%; mp: > 250 ºC; ^{1}H NMR (600 MHz, DMSO-d_6) δ 8.63 (s, 1H, quinolone-2-*H*), 7.97 (s, 1H, quinolone-5-*H*), 7.96 (s, 1H quinolone-8-*H*), 7.67 (s, 1H, thiazole-4-*H*), 6.95 (s, 2H, thiazole-2-NH_2), 4.38 (q, J = 6.9 Hz, 2H, CH_2CH$_3$), 3.53 (s, 4H, piperazine-3,3-*N*-(CH_2)$_2$), 3.00 (s, 4H, piperazine-2,2-*N*-(CH_2)$_2$), 1.44 (s, 9H, Boc-CH_3), 1.36 (t, J = 7.1 Hz, 3H, CH$_2$CH_3) ppm; ^{13}C NMR (151 MHz, DMSO-d_6) δ 173.1, 167.2, 154.5, 145.3, 144.7, 142.8, 134.8, 133.6, 126.6, 118.8, 117.3, 115.4, 104.2, 79.5, 51.7, 48.3, 28.6, 15.1 ppm; HRMS (ESI) calcd. for $C_{23}H_{28}ClN_5O_3S$ $[M + H]^+$, 490.1680; found, 490.1674.

*4.1.19. Synthesis of 3-(2-Aminothiazol-4-yl)-7-chloro-1-ethyl-6-(piperazin-1-yl)quinolin-4(1H)-one(**20**).*

A mixture of compound **19** (0.25 g, 1.02 mmol) and hydrochloric acid (1 mL) in dichloromethane (100 mL) was stirred at room temperature for 4 h. When the reaction was completed, the solvent was evaporated under reduced pressure. After chloroform was added, the resulting mixture was washed with aqueous solution of sodium hydroxide (3 × 20 mL). The organic extracts were dried over anhydrous sodium sulfate and concentrated. The crude product was purified *via* silica gel column chromatography (eluent, chloroform/methanol (V/V) = 15/1) to afford compound **20** (0.14 g) as yellow solid. Yield: 71.4%; mp: 241–243 ºC; ^{1}H NMR (600 MHz, DMSO-d_6) δ 8.63 (s, 1H, quinolone-2-*H*), 7.96 (s, 2H, quinolone-5-*H*, quinolone-8-*H*), 7.66 (s, 1H, thiazole-4-*H*), 6.94 (s, 2H, thiazole-2-NH_2), 4.39 (q, J = 7.1 Hz, 2H, CH_2CH$_3$), 3.01 (s, 4H, piperazine-2,2-*N*-(CH_2)$_2$), 2.98 (d, J = 3.5 Hz, 4H, piperazine-3,3-*N*-(CH_2)$_2$), 1.36 (t, J = 7.2 Hz, 3H, CH$_2$CH_3) ppm; ^{13}C NMR (151 MHz, DMSO-d_6) δ 173.2, 167.1, 145.8, 144.8, 142.8, 134.7, 133.6, 126.6, 118.9, 116.9, 115.4, 104.2, 52.3, 48.3, 45.7, 15.1 ppm; HRMS (ESI) calcd. for $C_{18}H_{20}ClN_5OS$ $[M + H]^+$, 390.1155; found, 390.1154.

*4.1.20. Synthesis of 3-(2-Aminothiazol-4-yl)-7-chloro-1-ethyl-6-(4-(2-oxopropyl)piperazin-1-yl)quinolin -4(1H)-one (**21**).*

Compound **21** was prepared according to the experimental procedure described for compound **15a** starting from 1-chloropropan-2- one (69.39 mg, 0.75 mmol), potassium carbonate (103.66 mg, 0.75 mmol) and compound **20** (194.95 mg, 0.50 mmol). The target compound **21** (163.45 mg) was obtained as yellow solid. Yield: 73.3%; mp: 248–250 ºC; ^{1}H NMR (600 MHz, DMSO-d_6) δ 8.63 (s, 1H, quinolone-2-*H*), 7.98 (s, 1H, quinolone-5-*H*), 7.95 (s, 1H, quinolone-8-*H*), 7.66 (s, 1H, thiazole-4-*H*), 6.94 (s, 2H, thiazole-2-NH_2), 4.38 (q, J = 7.1 Hz, 2H, CH_2CH$_3$), 3.28 (s, 2H, CH_2COCH$_3$), 3.06 (s, 4H, piperazine-2,2-*N*-(CH_2)$_2$), 2.65 (s, 4H, piperazine-3,3-*N*- (CH_2)$_2$), 2.12 (s, 3H, CH$_2$COCH_3), 1.36 (t, J = 7.1 Hz, 3H, CH$_2$CH_3) ppm; ^{13}C NMR (151 MHz, DMSO-d_6) δ 207.3, 173.2, 167.1, 145.5, 144.8, 142.8, 134.7, 133.5, 126.6, 118.9, 116.9, 115.4, 104.2, 67.7, 53.2, 51.7, 48.3, 28.1, 15.1 ppm; HRMS (ESI) calcd. for $C_{21}H_{24}ClN_5O_2S$ $[M + H]^+$, 446.1417; found, 446.1416.

*4.1.21. Synthesis of (E)-3-(2-Aminothiazol-4-yl)-7-chloro-1-ethyl-6-(4-(2-(hydroxyimino)propyl)piperazin -1-yl)quinolin-4(1H)-one (**22a**).*

Compound **22a** was prepared according to the experimental procedure described for compound **10a** starting from intermediate **21** (222.98 mg, 0.50 mmol), potassium carbonate (103.66 mg, 0.75 mmol) and hydroxylamine hydrochloride (52.11 mg, 0.75 mmol). The target compound **22a** (124.69 mg) was obtained as yellow solid. Yield: 54.2%; mp: > 250 ºC; ^{1}H NMR (600 MHz, DMSO-d_6) δ 10.55 (s, 1H, O*H*), 8.63 (s, 1H, quinolone-2-*H*), 7.98 (s, 1H, quinolone-5-*H*), 7.95 (s, 1H, quinolone-8-*H*), 7.66 (s, 1H, thiazole-4-*H*), 6.92 (s, 2H, thiazole-2-NH_2), 4.38 (q, *J* = 7.1 Hz, 2H, CH_2CH$_3$), 3.06 (s, 4H, piperazine-2,2-*N*-(CH_2)$_2$), 3.04 (s, 2H, CH_2C(N-OH)CH$_3$), 2.55 (s, 4H, piperazine-3,3-*N* -(CH_2)$_2$), 1.83 (s, 3H, -CH_3), 1.37 (d, *J* = 7.1 Hz, 3H, CH$_2$CH_3) ppm; ^{13}C NMR (151 MHz, DMSO-d_6) δ 173.2, 167.1, 145.5, 144.8, 142.8, 134.6, 133.5, 132.0, 129.1, 126.6, 118.9, 116.9, 115.4, 104.2, 62.2, 53.2, 51.8, 49.1, 48.3, 15.1, 12.7 ppm; HRMS (ESI) calcd. for $C_{21}H_{25}ClN_6O_2S$ $[M + H]^+$, 461.1526; found, 461.1524.

*4.1.22. Synthesis of (E)-3-(2-Aminothiazol-4-yl)-7-chloro-1-ethyl-6-(4-(2-(methoxyimino)propyl) piperazin-1-yl)quinolin-4(1H)-one (**22b**).*

Compound **22b** was prepared according to the experimental procedure described for compound **10a** starting from intermediate **21** (222.98 mg, 0.50 mmol), potassium carbonate (103.66 mg, 0.75 mmol) and *O*-methylhydroxylamine hydrochloride (62.64 mg, 0.75 mmol). The target compound **22b** (146.52 mg) was obtained as light yellow solid. Yield: 61.8%; mp: > 250 ºC; ^{1}H NMR (600 MHz, DMSO-d_6) δ 8.62 (s, 1H, quinolone-2-*H*), 7.98 (s, 1H, quinolone-5-*H*), 7.93 (s, 1H, quinolone-8-*H*), 7.66 (s, 1H, thiazole-4-*H*), 6.88 (s, 2H, thiazole-2-NH_2), 4.37 (q, *J* = 7.1 Hz, 2H, CH_2CH$_3$), 3.78 (s, 3H, OCH_3), 3.29 (s, 2H, CH_2C(N-OCH$_3$)CH$_3$), 3.06 (s, 4H, piperazine-2,2-*N*-(CH_2)$_2$), 2.56 (s, 4H, piperazine-3,3-*N*- (CH_2)$_2$), 1.85 (s, 3H, -CH_3), 1.36 (t, *J* = 7.1 Hz, 3H, CH$_2$CH_3) ppm; ^{13}C NMR (151 MHz, DMSO-d_6) δ 173.2, 167.1, 155.5, 145.5, 144.8, 142.8, 134.7, 133.5, 126.6, 118.9, 116.9, 115.4, 104.2, 61.7, 61.4, 53.2, 51.8, 49.1, 48.2, 15.0, 13.3 ppm; HRMS (ESI) calcd. for $C_{22}H_{27}ClN_6O_2S$ $[M + H]^+$, 475.1683; found, 475.1683.

*4.1.23. Synthesis of (E)-3-(2-Aminothiazol-4-yl)-7-chloro-1-ethyl-6-(4-(2-(4-fluorophenyl)-2-(methoxyimino)ethyl)piperazin-1-yl)quinolin- 4(1H)-one (**23a**).*

Compound **23a** was prepared according to the experimental procedure described for compound **15a** starting from intermediate **14a** (112.21 mg, 0.75 mmol), potassium carbonate (103.66 mg, 0.75 mmol) and compound **20** (194.55 mg, 0.50 mmol). The target compound **23a** (166.53 mg) was obtained as yellow solid. Yield: 60.1%; mp: 131–133 ºC; ^{1}H NMR (600 MHz, DMSO-d_6) δ 8.61 (s, 1H, quinolone-2-*H*), 7.94 (s, 1H, quinolone-5-*H*), 7.92 (s, 1H, quinolone-8-*H*), 7.86 (dd, *J* = 8.5, 5.7 Hz, 2H, 4-F-Ph-2,6-2*H*), 7.64 (s, 1H, thiazole-4-*H*), 7.24 (t, *J* = 8.8 Hz, 2H, 4-F-Ph-3,5-2*H*), 6.93 (s, 2H, thiazole-2-NH_2), 4.37 (dd, *J* = 13.6, 6.6 Hz, 2H, CH_2CH$_3$), 3.94 (s, 3H, -OCH_3), 3.72 (s, 2H, CH_2C(N-OCH$_3$), 2.97 (s, 4H, piperazine-2,2-*N*-(CH_2)$_2$), 2.63 (s, 4H, piperazine-3,3-*N*-(CH_2)$_2$), 1.35 (t, *J* = 7.0 Hz, 3H, CH$_2$CH_3) ppm; ^{13}C NMR (151 MHz, DMSO-d_6) δ 173.1, 167.1, 162.3, 153.9, 145.4, 144.8, 142.8, 134.7, 133.6, 131.9,

129.4, 126.6, 118.8, 116.9, 115.7, 115.6, 104.2, 62.3, 53.3, 51.7, 51.3, 48.2, 15.1 ppm; HRMS (ESI) calcd. for $C_{27}H_{28}ClFN_6O_2S$ $[M + H]^+$, 555.1745; found, 555.1741.

*4.1.24. Synthesis of (E)-3-(2-Aminothiazol-4-yl)-7-chloro-6-(4-(2-(4-chlorophenyl)-2-(methoxyimino)ethyl)piperazin-1-yl)-1-ethylquinolin-4(1H)-one (**23b**).*

Compound **23b** was prepared according to the experimental procedure described for compound **15a** starting from intermediate **14b** (162.75 mg, 0.75 mmol), potassium carbonate (103.66 mg, 0.75 mmol) and compound **20** (194.55 mg, 0.50 mmol). The target compound **23b** (181.59 mg) was obtained as yellow solid. Yield: 63.7%; mp: 244–246 ºC; ^{1}H NMR (600 MHz, DMSO-d_6) δ 8.61 (s, 1H, quinolone-2-*H*), 7.93 (s, 1H, quinolone-5-*H*), 7.92 (s, 1H, quinolone-8-*H*), 7.83 (s, 1H, 4-Cl-Ph-2-*H*), 7.82 (s, 1H, 4-Cl-Ph-6-*H*), 7.65 (s, 1H, thiazole-4-*H*), 7.47 (s, 1H, 4-Cl-Ph-3-*H*), 7.46 (s, 1H, 4-Cl-Ph-5-*H*), 6.91 (s, 2H, thiazole-2-NH_2), 4.37 (q, *J* = 7.0 Hz, 2H, CH_2CH$_3$), 3.95 (s, 3H, -OCH_3), 3.72 (s, 2H, CH_2C(N-OCH$_3$), 2.97 (s, 4H, piperazine-2,2-*N*-(CH_2)$_2$), 2.62 (s, 4H, piperazine-3,3-*N*-(CH_2)$_2$), 1.35 (t, *J* = 7.1 Hz, 3H, CH$_2$CH_3) ppm; ^{13}C NMR (151 MHz, DMSO-d_6) δ 173.1, 167.1, 153.9, 145.4, 144.8, 142.8, 134.7, 134.3, 133.6, 128.9, 128.7, 126.6, 118.8, 116.9, 115.4, 104.2, 62.4, 53.3, 51.7, 51.1, 48.2, 15.1 ppm; HRMS (ESI) calcd. for $C_{27}H_{28}Cl_2N_6O_2S$ $[M + H]^+$, 571.1450; found, 571.1445.

*4.1.25. Synthesis of (E)-3-(2-Aminothiazol-4-yl)-7-chloro-1-ethyl-6-(4-(2-(methoxyimino)-2-(4-methoxyphenyl)ethyl)piperazin-1-yl) quinolin -4(1H)-one (**23c**).*

Compound **23c** was prepared according to the experimental procedure described for compound **15a** starting from intermediate **14c** (159.79 mg, 0.75 mmol), potassium carbonate (103.66 mg, 0.75 mmol) and compound **20** (194.55 mg, 0.50 mmol). The target compound **23c** (170.71 mg) was obtained as light yellow solid. Yield: 60.3%; mp: 139–141 ºC; ^{1}H NMR (600 MHz, DMSO-d_6) δ 8.61 (s, 1H, quinolone-2-*H*), 7.93 (s, 2H, quinolone-5-*H*, quinolone-8-*H*), 7.75 (d, *J* = 8.8 Hz, 2H, 4-CH$_3$O-Ph-2,6-2*H*), 7.65 (s, 1H, thiazole-4-*H*), 6.96 (d, *J* = 8.8 Hz, 2H, 4-CH$_3$O-Ph-3,5-2*H*), 6.92 (s, 2H, thiazole-2-NH_2), 4.37 (q, *J* = 7.1 Hz, 2H, CH_2CH$_3$), 3.91 (s, 3H, -OCH_3), 3.79 (s, 3H, Ph-OCH_3), 3.69 (s, 2H, CH_2C(N-OCH$_3$), 2.98 (s, 4H, piperazine-2,2-*N*-(CH_2)$_2$), 2.63 (s, 4H, piperazine-3,3-*N*-(CH_2)$_2$), 1.35 (t, *J* = 7.1 Hz, 3H, CH$_2$CH_3) ppm; ^{13}C NMR (151 MHz, DMSO-d_6) δ 173.1, 167.1, 160.5, 154.2, 145.5, 144.8, 142.8, 134.7, 133.6, 128.5, 127.9, 126.6, 118.8, 116.9, 115.4, 114.1, 104.2, 62.1, 55.6, 53.3, 51.8, 51.2, 48.2, 15.1 ppm; HRMS (ESI) calcd. for $C_{28}H_{31}ClN_6O_3S$ $[M + H]^+$, 567.1945; found, 567.1935.

*4.1.26. Synthesis of (E)-3-(2-Aminothiazol-4-yl)-7-chloro-6-(4-(2-(2,4-dichlorophenyl)-2-(methoxyimino)ethyl)piperazin-1-yl)-1-ethylquinolin-4(1H)-one (**23d**).*

Compound **23d** was prepared according to the experimental procedure described for compound **15a** starting from intermediate **14e** (188.23 mg, 0.75 mmol), potassium carbonate (103.66 mg, 0.75 mmol) and compound **20** (194.55 mg, 0.50 mmol). The target compound **23d** (178.21 mg) was obtained as yellow solid. Yield: 59.0%; mp: 137–139 ºC; ^{1}H NMR (600 MHz, DMSO-d_6) δ 8.61 (s, 1H, quinolone-2-*H*), 7.92 (s, 1H, quinolone-5-*H*), 7.86 (s, 1H, quinolone-8-*H*), 7.68 (d, *J* = 1.9 Hz, 1H, 2,4-diCl-Ph-6-*H*), 7.64 (s, 1H,

thiazole-4-*H*), 7.50 (s, 1H, 2,4-diCl-Ph-3-*H*), 7.49 (d, *J* = 1.9 Hz, 1H, 2,4-diCl-Ph-5-*H*), 6.92 (s, 2H, thiazole-2-NH_2), 4.36 (q, *J* = 7.1 Hz, 2H, CH_2CH$_3$), 3.91 (s, 3H, -OCH_3), 3.68 (s, 2H, CH_2C(N-OCH$_3$)), 2.84 (s, 4H, piperazine-2,2-*N*-(CH_2)$_2$), 2.56 (s, 4H, piperazine-3,3-*N*-(CH_2)$_2$), 1.34 (t, *J* = 7.1 Hz, 3H, CH$_2$CH_3) ppm; ^{13}C NMR (151 MHz, DMSO-d_6) δ 173.1, 167.1, 156.7, 145.3, 144.8, 142.8, 134.7, 134.3, 134.0, 133.5, 132.8, 129.3, 127.5, 126.5, 118.8, 116.9, 115.4, 104.2, 62.4, 54.0, 53.5, 51.7, 48.2, 15.0 ppm; HRMS (ESI) calcd. for $C_{27}H_{27}Cl_3N_6O_2S$ $[M + H]^+$, 605.1060; found, 605.1027.

Acknowledgments

This work was partially supported by National Natural Science Foundation of China (Nos. 21672173, 21850410447, 21807008), China Postdoctoral Science Foundation (2018M633313), Chongqing Special Foundation for Postdoctoral Research Proposal (Nos. Xm2017184, XmT2018082), and Program for Overseas Young Talents from State Administration of Foreign Experts Affairs, China (Nos. WQ2017XNDX047, WQ20180083).

References

[1] (a) C. Gao, Y.L. Fan, F. Zhao, Q.C. Ren, X. Wu, L. Chang, F. Gao, Quinolone derivatives and their activities against methicillin-resistant *Staphylococcus aureus* (MRSA), Eur. J. Med. Chem. 157 (2018) 1081–1095;

(b) I.K.H. Poon, Y.H. Chiu, A.J. Armstrong, J.M. Kinchen, I.J. Juncadella, D.A. Bayliss, K.S. Ravichandran, Unexpected link between an antibiotic, pannexin channels and apoptosis, Nature 507 (2014) 329–334.

[2] (a) I. Laponogov, M.K. Sohi, D.A. Veselkov, X.S. Pan, R. Sawhney, A.W. Thompson, K.E. McAuley, L.M. Fisher, M.R. Sanderson, Structural insight into the quinolone-DNA cleavage complex of type IIA topoisomerases, Nat. Struct. Mol. Biol. 16 (2009) 667–669;

(b) P.G. Higgins, A.C. Fluit, F.J. Schmitz, Fluoroquinolones: Structure and target sites, Curr. Drug Targets 4 (2003) 181–190;

(c) K.M.G. O'Connell, J.T. Hodgkinson, H.F. Sore, M. Welch, G.P.C. Salmond, D.R. Spring, Combating multidrug-resistant bacteria: Current strategies for the discovery of novel antibacterials, Angew. Chem. Int. Ed. 52 (2013) 10706–10733;

(d) B.D. Bax, P.F. Chan, D.S. Eggleston, A. Fosberry, D.R. Gentry, F. Gorrec, I. Giordano, M.M. Hann, A. Hennessy, M. Hibbs, J.Z. Huang, E. Jones, J. Jones, K.K. Brown, C.J. Lewis, E.W. May, M.R. Saunders, O. Singh, C.E. Spitzfaden, C. Shen, A. Shillings, A.J. Theobald, A. Wohlkonig, N.D. Pearson, M.N. Gwynn, Type IIA topoisomerase inhibition by a new class of antibacterial agents, Nature 466 (2010) 935–940;

(e) G.S. Bisacchi, Origins of the quinolone class of antibacterials: An expanded “discovery story”, J. Med. Chem. 58 (2015) 4874–4882.

[3] C.Y. Kao, H.M. Wu, W.H. Lin, C.C. Tseng, J.J. Yan, M.C. Wang, C.H. Teng, J.J. Wu, Plasmid-mediated quinolone resistance determinants in quinolone-resistant *Escherichia coli* isolated from patients with bacteremia in a university hospital in Taiwan, 2001–2015, Sci. Rep. 6 (2016) 32281–32289.

[4] (a) Y.Q. Hu, S. Zhang, Z. Xu, Z.S. Lv, M.L. Liu, L.S. Feng, 4-Quinolone hybrids and their antibacterial activities, Eur. J. Med. Chem. 141 (2017) 335–345;

(b) G.F. Zhang, S. Zhang, B.F. Pan, X.F. Liu, L.S. Feng, 4-Quinolone derivatives and their activities against Gram positive pathogens, Eur. J. Med. Chem. 143 (2018) 710–723.

[5] (a) F. Gao, P. Wang, H. Yang, Q. Miao, L. Ma, G.M. Lu, Recent developments of quinolone-based derivatives and their activities against *Escherichia coli*, Eur. J. Med. Chem. 157 (2018) 1223–1248;

(b) X.M. Chu, C. Wang, W. Liu, L.L. Liang, K.K. Gong, C.Y. Zhao, K.L. Sun, Quinoline and quinolone dimers and their biological activities: An overview, Eur. J. Med. Chem. 161 (2019) 101–117.

[6] (a) L.A. Mitscher, Bacterial topoisomerase inhibitors: Quinolone and pyridone antibacterial agents, Chem. Rev. 105 (2005) 559–592;

(b) I.K.H. Poon, Y.H. Chiu, A.J. Armstrong, J.M. Kinchen, I.J. Juncadella, D.A. Bayliss, K.S. Ravichandran, Unexpected link between an antibiotic, pannexin channels and apoptosis, Nature 507 (2014) 329–334.

[7] W.W. Gao, C.H. Zhou, Antimicrobial 2-aminothiazolyl quinolones: What is their potential in the clinic? Future Med. Chem. 9 (2017) 1461–1464.

[8] (a) K.C. Fang, Y.L. Chen, J.Y. Sheu, T.C. Wang, C.C. Tzeng, Synthesis, antibacterial, and cytotoxic evaluation of certain 7-substituted norfloxacin derivatives, J. Med. Chem. 43 (2000) 3809–3812;

(b) L. Zhang, K.V. Kumar, R.X. Geng, C.H. Zhou, Design and biological evaluation of novel quinolone-based metronidazole derivatives as potent Cu^{2+} mediated DNA-targeting antibacterial agents, Bioorg, Med. Chem. Lett. 25 (2015) 3699–3705;

(c) L. Zhang, D. Addla, J. Ponmani, A. Wang, D. Xie, Y.N. Wang, S.L. Zhang, R.X. Geng, G.X. Cai, S. Li, C.H. Zhou, Discovery of membrane active benzimidazole quinolones-based topoisomerase inhibitors as potential DNA-binding antimicrobial agents, Eur. J. Med. Chem. 111 (2016) 160–182.

[9] (a) L. Zhang, X.M. Peng, G.L.V. Damu, R.X. Geng, C.H. Zhou, Comprehensive review in current developments of imidazole-based medicinal chemistry, Med. Res. Rev. 34 (2014) 340–437;

(b) C.H. Zhou, Y. Wang, Recent researches in triazole compounds as medicinal drugs, Curr. Med. Chem. 19 (2012) 239–280.

(c) Z.Z. Li, S.K. Maddili, V.K.R. Tangadanchu, R.R.Y. Bheemanaboina, J.M. Lin, R.G. Yang, G.X. Cai, C.H. Zhou, Researches and applications of nitroimidazole heterocycles in medicinal chemistry, Sci. Sin. Chim. 49 (2019) 230–255.

[10] (a) X.M. Peng, G.X. Cai, C.H. Zhou, Recent developments in azole compounds as antibacterial and antifungal agents, Curr. Top. Med. Chem. 13 (2013) 1963–2010;

(b) X.M. Peng, G.L.V. Damu, C.H. Zhou, Current developments of coumarin compounds in medicinal chemistry, Curr. Pharm. Des. 19 (2013) 3884–3930.

[11] (a) Y.N. Wang, R.R.Y. Bheemanaboina, W.W. Gao, J. Kang, G.X. Cai, C.H. Zhou, Discovery of benzimidazole-quinolone hybrids as new cleaving agents toward drug-resistant *Pseudomonas ae*ruginosa DNA, ChemMedChem 13 (2018) 1004–1017;

(b) L. Zhang, K.V. Kumer, S. Rasheed, R.X. Geng, C.H. Zhou, Design, synthesis, and antimicrobial evaluation of novel quinolone imidazoles and interactions with MRSA DNA, Chem. Biol. Drug Des. 86 (2015) 648–655;

(c) S.F. Cui, L.P. Peng, H.Z. Zhang, S. Rasheed, K.V. Kumer, C.H. Zhou, Novel hybrids of metronidazole and quinolones: Synthesis, bioactive evaluation, cytotoxicity, preliminary antimicrobial mechanism and effect of metal ions on their transportation by human serum albumin, Eur. J. Med. Chem. 86 (2014) 318–334;

[12] (a) G.S. Basarab, P.J. Hill, C.E. Garner, K. Hull, O. Green, B.A. Sherer, P.B. Dangel, J.I. Manchester, S. Bist, S. Hauck, F. Zhou, M. Uria-Nickelsen, R. Illingworth, R. Alm, M. Rooney, A.E. Eakin, Optimization of pyrrolamide topoisomerase II inhibitors toward identification of an antibacterial clinical candidate (AZD5099), J. Med. Chem. 57 (2014) 6060–6082;

(b) Y.Y. Chen, L. Gopala, R.R.Y. Bheemanaboina, H.B. Liu, Y. Cheng, R.X. Geng, C.H. Zhou, Novel naphthalimide aminothiazoles as potential multitargeting antimicrobial agents, ACS Med. Chem. Lett. 8 (2017) 1331–1335.

[13] (a) J. Tomberg, M. Unemo, C. Davies, R.A. Nicholas, Molecular and structural analysis of mosaic variants of penicillin-binding protein 2 conferring decreased susceptibility to expanded-spectrum cephalosporins in neisseria gonorrhoeae: Role of epistatic mutations, Biochemistry 49 (2010) 8062–8070;

(b) D.L. Hughes, Patent review of manufacturing routes to fifth-generation cephalosporin drugs. part 2, ceftaroline fosamil and ceftobiprole medocaril, Org. Process Res. Dev. 21 (2017) 800–815;

(c) H. Dai, S.S. Ge, G. Li, J. Chen, Y.J. Shi, L.Y. Ye, Y. Ling, Synthesis and bioactivities of novel pyrazole oxime derivatives containing a 1,2,3-thiadiazole moiety, Bioorg. Med. Chem. Lett. 26 (2016) 4504–4507.

[14] (a) K. Lv, M.L. Liu, L.S. Feng, L.Y. Sun, Y.X. Sun, Z.Q. Wei, H.Q. Guo, Synthesis and antibacterial activity of naphthyridone derivatives containing mono/difluoro-methyloxime pyrrolidine scaffolds, Eur. J. Med. Chem. 47 (2012) 619–625;

(b) H.M. Liu, J. Huang, J.Y. Wang, M.H. Wang, M.L. Liu, B. Wang, H.Y. Guo, Y. Lu, Synthesis, antimycobacterial and antibacterial evaluation of l-[(1R, 2S)-2-fluorocyclopropyl]fluoroquinolone derivatives containing an oxime functional moiety, Eur. J. Med. Chem. 86 (2014) 628–638.

[15] (a) H.S. Park, H.J. Kim, M.J. Seol, D.R. Choi, E.C. Chio, J.H. Kwak, *In vitro* and *in vivo* antibacterial activities of DW-224a, a new fluoronaphthyridone, Antimicrob. Agents Chemother. 50 (2006) 2261–2264;

(b) H.J. Yun, Y.H. Min, J.A. Lim, J.W. Kang, S.Y. Kim, M.J. Kim, J.H. Jeong, Y.J. Choi, H.J. Kwon, Y.H. Jung, M.S. Shim, E.C. Choi, *In vitro* and *in vivo* antibacterial activities of DW286, a new fluoronaphthyridone antibiotic, Antimicrob. Agents Chemother. 46 (2002) 3071–3074.

[16] M. Shaquiquzzaman, G. Verma, A. Marella, M. Akhter, W. Akhtar, M.F. Khan, S. Tasneem, M.M. Alam, Piperazine scaffold: A remarkable tool in generation of diverse pharmacological agents, Eur. J. Med. Chem. 102 (2015) 487–529.

[17] (a) R. Neelarapu, J.R. Maignan, C.L. Lichorowic, A. Monastyrskyi, T.S. Mutka, A.N. LaCrue, L.D. Blake, D. Casandra, S. Mashkouri, J.N. Burrows, P.A. Willis, D.E. Kyle, R. Manetsch, Design and synthesis of orally bioavailable piperazine substituted 4(1*H*)-quinolones with potent antimalarial activity: Structure-activity and structure-property relationship studies, J. Med. Chem. 61 (2018) 1450–1473;

(b) L.L. Wang, N. Battini, R.R.Y. Bheemanaboina, S.L. Zhang, C.H. Zhou, Design and synthesis of aminothiazolyl

norfloxacin analogues as potential antimicrobial agents and their biological evaluation. Eur. J. Med. Chem. 167 (2019) 105–123.

[18] (a) S.F. Cui, D. Addla, C.H. Zhou, Novel 3-aminothiazolquinolones: Design, synthesis, bioactive evaluation, SARs, and preliminary antibacterial mechanism. J. Med. Chem. 59 (2016) 4488–4510;

(b) Y. Cheng, S.R. Avula, W.W. Gao, D. Addla, V.K.R. Tangadanchu, L. Zhang, J.M. Lin, C.H. Zhou, Multi-targeting exploration of new 2-aminothiazolyl quinolones: Synthesis, antimicrobial evaluation, interaction with DNA, combination with topoisomerase IV and penetrability into cells, Eur. J. Med. Chem. 124 (2016) 935–945.

[19] Methods for Dilution Antimicrobial Susceptibility Tests for Bacteria that Grow Aerobically, seventh ed.; National Committee for Clinical Laboratory Standards: Wayne, PA, 2006, M7–A7.

[20] (a) P. Jeyakkumar, L. Zhang, S.R. Avula, C.H. Zhou, Design, synthesis and biological evaluation of berberine-benzimidazole hybrids as new type of potentially DNA-targeting antimicrobial agents, Eur. J. Med. Chem. 122 (2016) 205–215;

(b) J.S. Lv, X.M. Peng, B. Kishore, C.H. Zhou, 1,2,3-Triazole-derived naphthalimides as a novel type of potential antimicrobial agents: Synthesis, antimicrobial activity, interaction with calf thymus DNA and human serum albumin, Bioorg. Med. Chem. Lett. 24 (2014) 308–313.

[21] (a) W.W. Gao, S. Rasheed, V.K.R. Tangadanchu, Y. Sun, X.M. Peng, Y. Cheng, F.X. Zhang, J.M. Lin, C.H. Zhou, Design, synthesis and biological evaluation of amino organophosphorus imidazoles as a new type of potential antimicrobial agents, Sci. China Chem. 60 (2017) 769–785;

(b) W.W. Gao, L. Gopala, R.R.Y. Bheemanaboina, G.B. Zhang, S. Li, C.H. Zhou, Discovery of 2-aminothiazolyl berberine derivatives as effectively antibacterial agents toward clinically drug-resistant Gram-negative *Acinetobacter baumanii*, Eur. J. Med. Chem. 146 (2018) 15–37.

[22] Y. Zhang, V.K.R. Tangadanchu, R.R.Y. Bheemanaboina, Y. Cheng, C.H. Zhou, Novel carbazole-triazole conjugates as DNA-targeting membrane active potentiators against clinical isolated fungi, Eur. J. Med. Chem. 155 (2018) 579–589.

[23] (a) M.M. Konai, C. Ghosh, V. Yarlagadda, S. Samaddar, J. Haldar, Membrane-active phenylalanine-conjugated lipophilic norspermidine derivatives with selective antibacterial activity, J. Med. Chem. 57 (2014) 9409–9423;

(b) Y.Y. Hu, R.R.Y. Bheemanaboina, N. Battini, C.H. Zhou, Sulfonamide-derived four-component molecular hybrids as novel DNA-targeting membrane active potentiators against clinical *Escherichia coli*, Mol. Pharm. 16 (2019) 1036–1052.

[24] A. Adan, Y. Kiraz, Y. Baran, Cell proliferation and cytotoxicity assays, Curr. Pharm. Biotechno. 17 (2016) 1213–1221.

[25] Y. Zhang, V.K.R. Tangadanchu, Y. Cheng, R.G. Yang, J.M. Lin, C.H. Zhou, Potential antimicrobial isopropanol-conjugated carbazole azoles as dual targeting inhibitors of *Enterococcus faecalis*, ACS Med. Chem. Lett. 9 (2018) 244–249.

[26] G.B. Zhang, S.K.V. Maddili, K.R. Tangadanchu, L. Gopala, W.W. Gao, G.X. Cai, C.H. Zhou, Discovery of natural berberine-derived nitroimidazoles as potentially multi-targeting agents against drug-resistant *Escherichia coli*, Sci. China Chem. 61 (2018) 557–568.

[27] (a) M. Gjorgjieva, T. Tomasic, M. Barancokova, S. Katsamakas, J. Ilas, P. Tammela, L.P. Masic, D. Kikelj, Discovery of benzothiazole scaffold-based DNA gyrase B inhibitors, J. Med. Chem. 59 (2016) 8941–8954;

(b) W. Hu, X.S. Huang, J.F. Wu, L. Yang, Y.T. Zheng, Y.M. Shen, Z.Y. Li, X. Li, Discovery of novel topoisomerase II inhibitors by medicinal chemistry approaches, J. Med. Chem. 61 (2018) 8947–8980.

[28] (a) Y.N. Wang, R.R.Y. Bheemanaboina, G.X. Cai, C.H. Zhou, Novel purine benzimidazoles as antimicrobial agents by regulating ROS generation and targeting clinically resistant *Staphylococcus aureus* DNA groove, Bioorg. Med. Chem. Lett. 28 (2018) 1621–1628;

(b) X.M. Peng, L.P. Peng, S. Li, S.R. Avula, K.V. Kumar, S.L. Zhang, K.Y. Tam, C.H. Zhou, Quinazolinone azolyl ethanols: Potential lead antimicrobial agents with dual action modes targeting MRSA DNA, Future Med. Chem. 8 (2016) 1927–1940.

[29] (a) P. Pomastowski, M. Sprynskyy, P. Žuvela, K. Rafinska, M. Mi-lanowski, J.J. Liu, M. Yi, B. Buszewski, Silver-lactoferrin nanocomplexes as a potent antimicrobial agent, J. Am. Chem. Soc. 138 (2016) 7899–7909;

(b) Y.G. Zheng, M. Zheng, X. Ling, Y. Liu, Y.S. Xue, L. An, N. Gu, M. Jin, Design, synthesis, quantum chemical studies and biological activity evaluation of pyrazole-benzimidazole derivatives as potent Aurora A/B kinase inhibitors, Bioorg. Med. Chem. Lett. 23 (2013) 3523–3530.

[30] (a) Y. Shimazaki, J. Tanaka, Y. Kohara, M. Kamahori, T. Sakamoto, Parallel evaluation of melting temperatures of DNAs in the arrayed droplets through the fluorescence from DNA intercalators, Anal. Chem. 89 (2017) 6305–6308;

(b) D. Addla, S.Q. Wen, W.W. Gao, S.K. Maddili, L. Zhang, C.H. Zhou, Design, synthesis, and biological evaluation of novel carbazole aminothiazoles as potential DNA targeting antimicrobial agents, Med. Chem. Commun. 7 (2016) 1988–1994.

[31] (a) S. Narva, S. Chitti, B.R. Bala, M. Alvala, N. Jain, V.G.C.S. Kondapalli, Synthesis and biological evaluation of pyrrolo[2,3-b]pyridine analogues as antiproliferative agents and their interaction with calf thymus DNA, Eur. J. Med. Chem. 114 (2016) 220–231;

(b) B.T. Yin, C.Y. Yan, X.M. Peng, S.L. Zhang, S. Rasheed, R.X. Geng, C.H. Zhou, Synthesis and biological evaluation of a-triazolyl chalcones as a new type of potential antimicrobial agents and their interaction with calf thymus DNA and human serum albumin, Eur. J. Med. Chem. 71 (2014) 148–159;

(c) H.Z. Zhang, J.M. Lin, S. Rasheed, C.H. Zhou, Design, synthesis, and biological evaluation of novel benzimidazole derivatives and their interaction with calf thymus DNA and synergistic effects with clinical drugs, Sci. China Chem. 57 (2014) 807–822.

[32] (a) X.J. Fang, P. Jeyakkumary, S.R. Avula, Q. Zhou, C.H. Zhou, Design, synthesis and biological evaluation of 5-fluorouracil-derived benzimidazoles as novel type of potential antimicrobial agents, Bioorg. Med. Chem. Lett. 26 (2016) 2584–2588;

(b) L.L. Dai, H.Z. Zhang, S. Nagarajan, S. Rasheed, C.H. Zhou, Synthesis of tetrazole compounds as a novel type of potential antimicrobial agents and their synergistic effects with clinical drugs and interactions with calf thymus DNA, Med. Chem. Commun. 6 (2015) 147–154.

[33] (a) D. Li, R.R.Y. Bheemanaboina, N. Battini, V.K.R. Tangadanchu, X.F. Fang, C.H. Zhou, Novel organophosphorus aminopyrimidines as unique structural DNA-targeting membrane active inhibitors towards drug-resistant methicillin-resistant *Staphylococcus aureus*, Med. Chem. Commun. 9 (2018) 1529–1537;

(b) J. Kang, L. Gopala, V.K.R. Tangadanchu, W.W. Gao, C.H. Zhou, Novel naphthalimide nitroimidazoles as multitargeting antibacterial agents against resistant *Acinetobacter baumannii*, Future Med. Chem. 10 (2018) 711–724.

[34] X.F. Fang, D. Li, V.K.R. Tangadanchu, L. Gopala, W.W. Gao, C.H. Zhou, Novel potentially antifungal hybrids of 5-flucytosine and fluconazole: Design, synthesis and bioactive evaluation, Bioorg. Med. Chem. Lett. 27 (2017) 4964–4969.

[35] (a) G. Zhang, P. Fu, L. Wang, M. Hu, Molecular spectroscopic studies of farrerol interaction with calf thymus DNA, J. Agric. Food Chem. 59 (2011) 8944–8952;

(b) S.K. Maddili, Z.Z. Li, V.K. Kannekanti, R.R.Y. Bheemanaboina, B. Tuniki, V.K.R. Tangadanchu, C.H. Zhou, Azoalkyl ether imidazo[2,1-*b*]benzothiazoles as potentially antimicrobial agents with novel structural skeleton, Bioorg. Med. Chem. Lett. 28 (2018) 2426–2431.

[36] (a) N. Ibrahim, H. Ibrahim, S. Kim, J.P. Nallet, F. Nepveu, Interactions between antimalarial indolone-N-oxide derivatives and human serum albumin, Biomacromolecules 11 (2010) 3341–3351.

(b) H. Sun, M.F. Ansari, N. Battini, R.R.Y. Bheemanaboina, C.H. Zhou, Novel potential artificial MRSA DNA intercalators: Synthesis and biological evaluation of berberine derived thiazolidinediones, Org. Chem. Front. 6 (2019) 319–334.

[37] (a) B. Noverges, M. Medio-Simn, G. Asensioa, Palladium-catalyzed suzuki carbonylative reaction of α-halomethyl oxime ethers: A regioselective route to unsymmetrical 1,3-oxyiminoketones, Adv. Synth. Catal. 356 (2014) 3649–3658;

(b) Y. Wang, G.L.V. Damu, J.S. Lv, R.X. Geng, D.C. Yang, C.H. Zhou, Design, synthesis and evaluation of clinafloxacin triazole hybrids as a new type of antibacterial and antifungal agents, Bioorg. Med. Chem. Lett. 22 (2012) 5363–5366.

Lists of table and scheme captions

Table 1 MIC values (mM) for aminothiazolyl quinolone oximes against Gram-positive bacteria and Gram-negative bacteria.[a]

Compds	Gram-positive bacteria					Gram-negative bacteria					
	MRSA	*E. F.*	*S. A.*	*S. A.* 25923	*S. A.* 29213	*K. P.*	*E. C.*	*E. C.* 25922	*P. A.*	*P. A.* 27853	*A. B.*
9	0.072	0.288	0.144	0.288	0.575	0.072	1.150	0.288	0.288	0.036	0.288
10a	0.072	0.288	0.072	0.036	0.144	0.072	0.288	0.072	0.288	0.144	0.288
10b	0.009	0.070	0.035	0.017	0.140	0.070	0.070	0.035	0.070	0.035	0.279
10c	0.135	0.068	0.034	0.135	0.068	0.135	0.135	0.068	0.135	0.135	0.135
10d	0.066	0.526	0.263	0.132	0.263	0.526	0.263	0.263	0.263	0.132	0.263
11	0.424	0.424	0.848	0.848	0.848	0.848	0.424	0.848	0.848	0.848	0.848
15a	0.238	0.475	0.475	0.238	0.475	0.951	0.475	0.951	0.951	0.951	0.951
15b	0.029	0.115	0.231	0.058	0.231	0.231	0.231	0.461	0.231	0.058	0.115
15c	0.465	0.232	0.465	0.465	0.465	0.465	0.465	0.232	0.465	0.465	0.465
15d	0.434	0.434	0.217	0.054	0.217	0.217	0.109	0.869	0.217	0.217	0.054
15e	0.230	0.460	0.460	0.460	0.460	0.460	0.460	0.460	0.460	0.460	0.460
22a	0.139	0.139	0.035	0.017	0.139	0.139	0.069	0.278	0.139	0.555	0.278
22b	0.067	0.135	0.067	0.135	0.135	0.135	0.269	0.269	0.269	0.135	0.135
23a	0.014	0.058	0.029	0.058	0.058	0.231	0.014	0.058	0.461	0.058	0.115
23b	0.224	0.448	0.224	0.224	0.224	0.448	0.448	0.448	0.448	0.448	0.448
23c	0.451	0.451	0.451	0.451	0.451	0.451	0.451	0.451	0.451	0.451	0.451
23d	0.211	0.211	0.422	0.422	0.211	0.422	0.422	0.422	0.422	0.422	0.422
A [b]	0.050	0.025	0.025	0.025	0.012	0.025	0.099	0.050	0.099	0.025	0.050
B [b]	0.025	0.013	0.006	0.003	0.003	0.013	0.050	0.025	0.006	0.002	0.025

[a]MRSA, *Methicillin-resistant Staphylococcus aureus* (N315); *E. F.*, *Enterococcus faecalis*; *S. A.*, *Staphylococcus aureus*; *S. A.* ATCC 25923, *Staphylococcus aureus* ATCC 25923; *S. A.* ATCC 29213, *Staphylococcus aureus* ATCC 29213; *K. P.*, *Klebsiella pneumoniae*; *E. C.*, *Escherichia coli*; *E. C.* ATCC 25922, *Escherichia coli* ATCC 25922; *P. A.*, *Pseudomonas aeruginosa*; *P. A.* ATCC 27853, *Pseudomonas aeruginosa* ATCC 27853; *A. B.*, *Acinetobacter baumannii*. [b] **A** = Chloromycin, **B** = Norfloxacin.

Table 2 Combination effects of *O*-methyl oxime derivative **10b** with reference drugs.[a] (MIC = 10^{-3}mM)

Microbia	MRSA	*S. aureus*	*K. pneumoniae*	*C. albicans*	*C. tropicals*
Compds	**C/10b**	**C/10b**	**C/10b**	**F/10b**	**F/10b**
$MIC_{RD/\mathbf{10b}}$	31.52/8.72	31.52/34.89	15.76/69.78	13.06/69.78	26.12/69.78
$MIC_{Mixture}$	3.94/4.36	7.88/8.72	7.88/8.72	3.26/2.18	26.12/17.44
FIC^{b}_{Index}	0.625	0.5	0.625	0.281	1.25
Effect	Synergistic	Synergistic	Synergistic	Synergistic	Additive

[a]RD, Reference Drugs; C, Cefixime; F, Fluconazole; [b]The fractional inhibitory concentration index (FIC) = (MIC of compound A combined/MIC of compound A alone) + (MIC of compound B combined/ MIC of compound B alone). FIC index ≤ 1, synergistic effect; 1 < FIC index ≤ 2, additive effect; FIC index > 2, antagonistic effect.

Table 3 Plots of HOMO, LUMO and their energy gaps (in eV) for compounds **10b**, **15b** and **23a**.

Compds	HOMOs	Energy gaps	LUMOs
10b	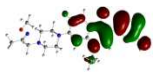	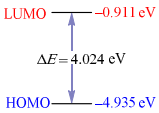	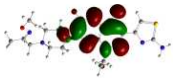
15b	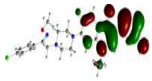	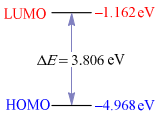	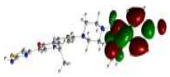
23a	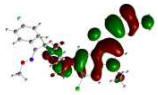	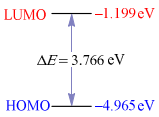	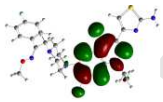

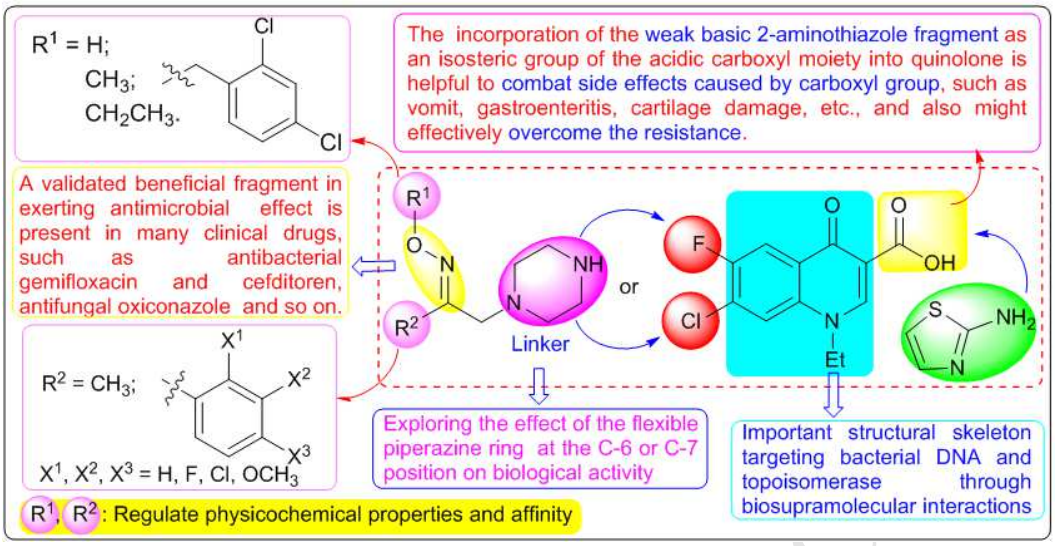

Fig. 1 Design of novel hybrids of quinolone, aminothiazole, piperazine and oxime fragments.

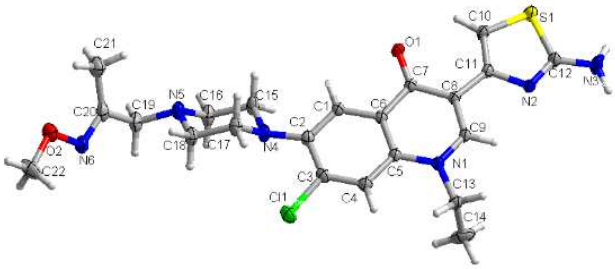

Fig. 2 Crystal structure of *O*-methyl oxime derivative **22b**.

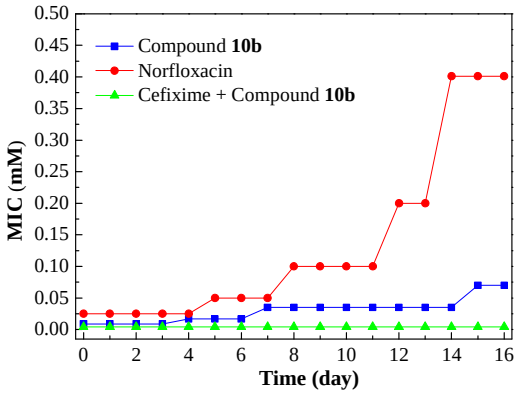

Fig. 3 The resistance development of active molecule **10b** against MRSA strain.

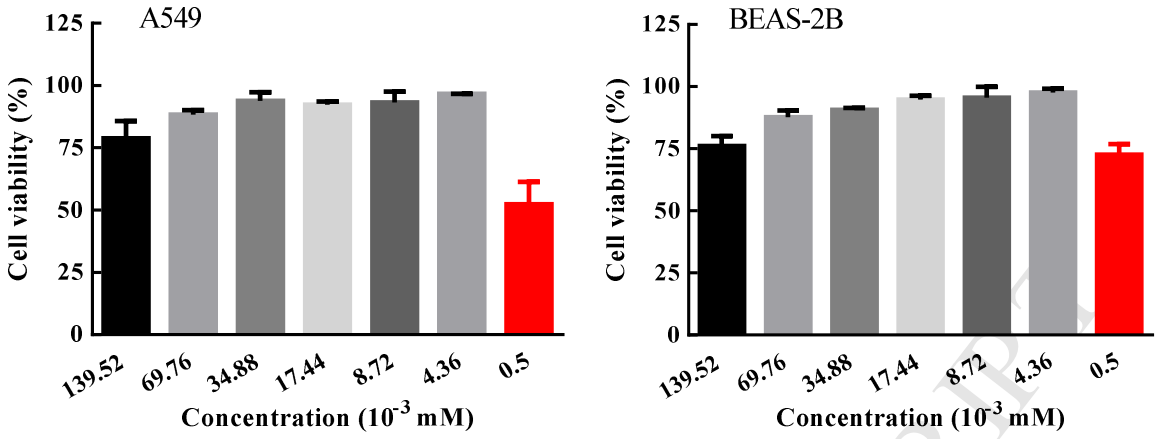

Fig. 4 The viabilities of A549 and BEAS-2B cell lines after being exposed to molecule **10b** tested by MTT assay. The standard deviation from three independent experiments was plotted.

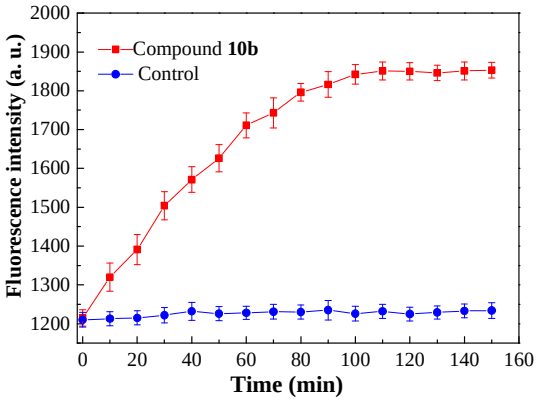

Fig. 5 Membrane permeabilization of molecule **10b** toward MRSA.

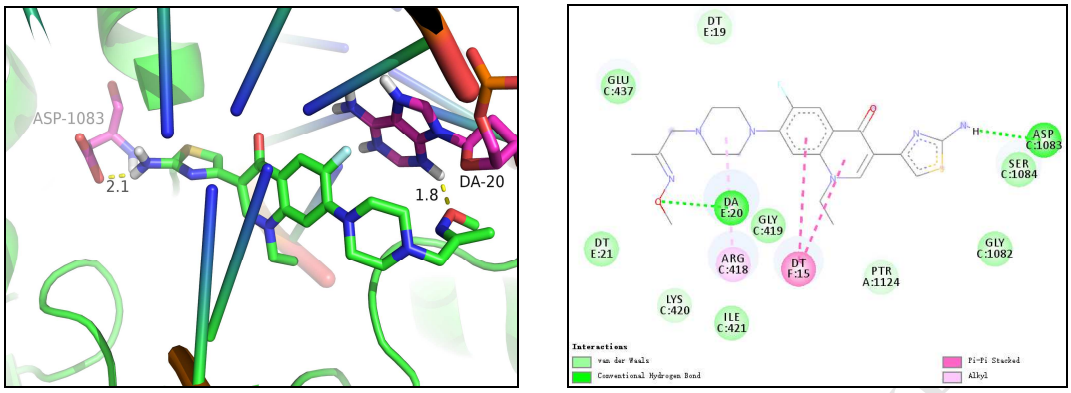

Fig. 6 (A) Three-dimensional supramolecular conformations of molecule **10b** docked in topoisomerase IV–DNA complex; (B) Two-dimensional supramolecular conformation of molecule **10b** docked in topoisomerase IV–DNA complex.

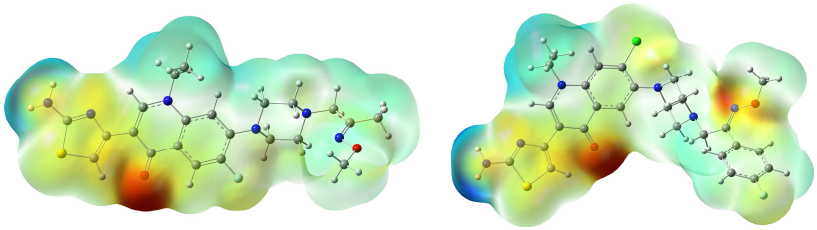

Fig. 7 MEP surfaces of *O*-methyl oxime derivatives **10b** (left) and **23a** (right).

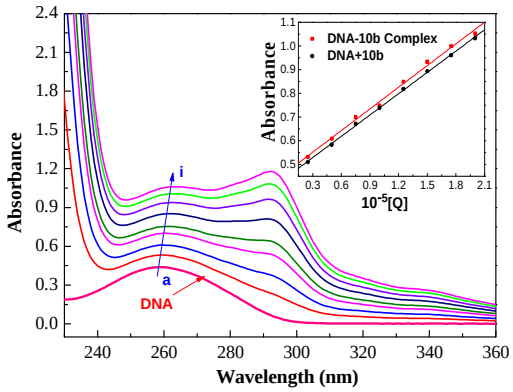

Fig. 8 UV absorption spectra of DNA with active molecule **10b** at different concentrations (pH = 7.4, T = 290 K). Inset: comparison of absorption at 260 nm between the compound **10b**–DNA complex and the sum values of free DNA and free compound **10b**. *c*(DNA) = 7.20 × 10^{-5} mol/L, and *c*(compound **10b**) = 0–2.0 × 10^{-5} mol/L for curves *a*–*i* respectively at increment 0.25 × 10^{-5}.

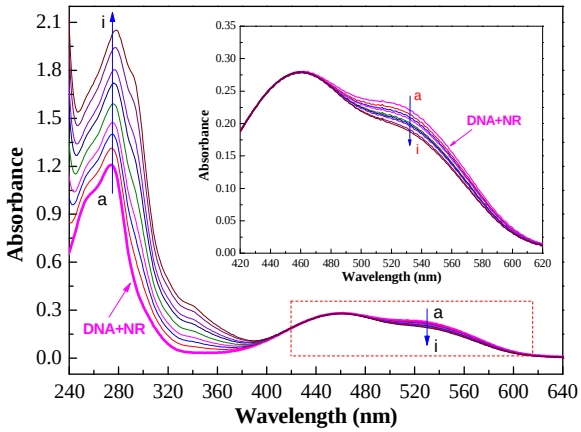

Fig. 9 UV absorption spectra of the competitive supramolecular binding between **10b** and NR with DNA. *c*(DNA) = 7.20 × 10^{-5} mol/L, *c*(NR) = 2 × 10^{-5} mol/L, and *c*(compound **10b**) = 0–2.00 × 10^{-5} mol/L for curves *a*–*i* respectively at increment 0.25 × 10^{-5} mol/L. (Inset) Absorption spectra of the system with the increasing concentration of **10b** in the wavelength range of 375–600 nm absorption spectra of competitive reaction between compound **10b** and NR with DNA.

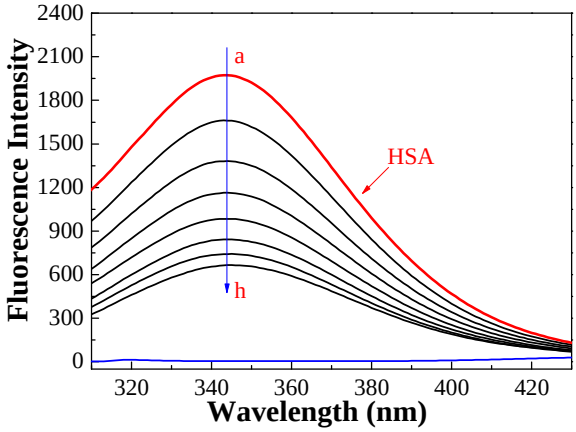

Fig. 10 Emission spectra of HSA in presence of various concentrations of compound **10b** (T = 298 K, E_{ex} = 285 nm). *c*(HSA) = 1.0 × 10^{-5} mol/L; *c*(compound **10b**) = 0–1.167 × 10^{-5} mol/L for curves *a*–*h* respectively at increment 0.1667 × 10^{-5} mol/L.

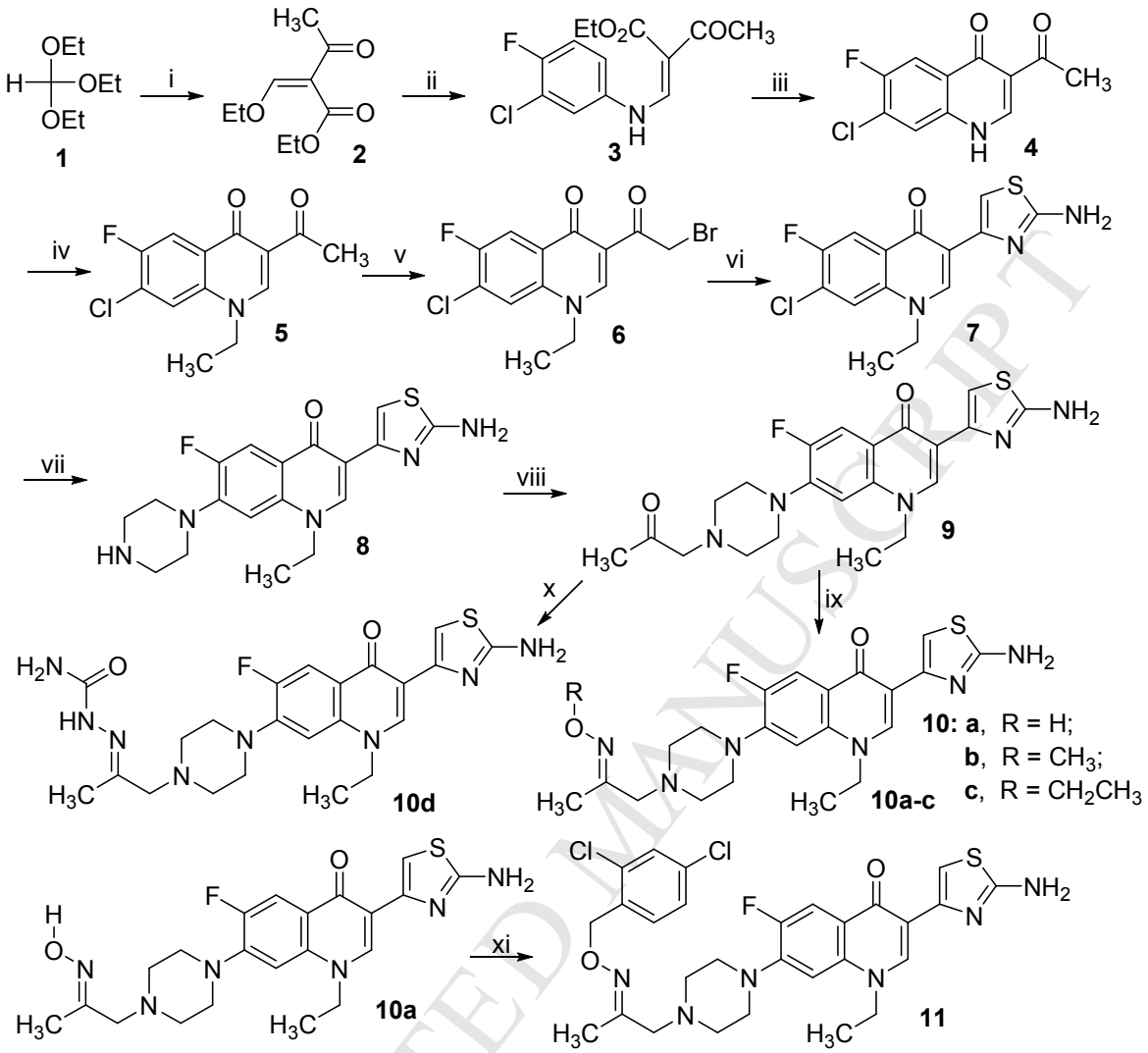

Scheme 1 Synthetic route of aminothiazolquinolone oximes **10a–c**, **11** and imine derivative **10d**. Reagents and conditions: (i) ethyl acetoacetate, acetic anhydride, 130 ºC, 2 h; (ii) 3-chloro-4-fluoroaniline, 130 ºC, 30 min; (iii) Ph_2O, reflux, 250 ºC, 1 h; (iv) bromoethane, K_2CO_3, MeCN, 80 ºC, 12 h; (v) Br_2, acetic acid, 60 ºC, 8 h; (vi) thiourea, EtOH, 80 ºC, 4 h; (vii) NMP, piperazine, 130 ºC, 24 h; (viii) 1-chloropropan-2-one, K_2CO_3, MeCN, 80 ºC, 6 h; (ix) alkoxyamine hydrochloride, K_2CO_3, MeCN, 80 ºC, 8 h; (x) aminourea hydrochloride, K_2CO_3, MeCN, 80 ºC, 8 h; (xi) 2,4-dichlorobenzylchloride, K_2CO_3, MeCN, 80 ºC, 12 h.

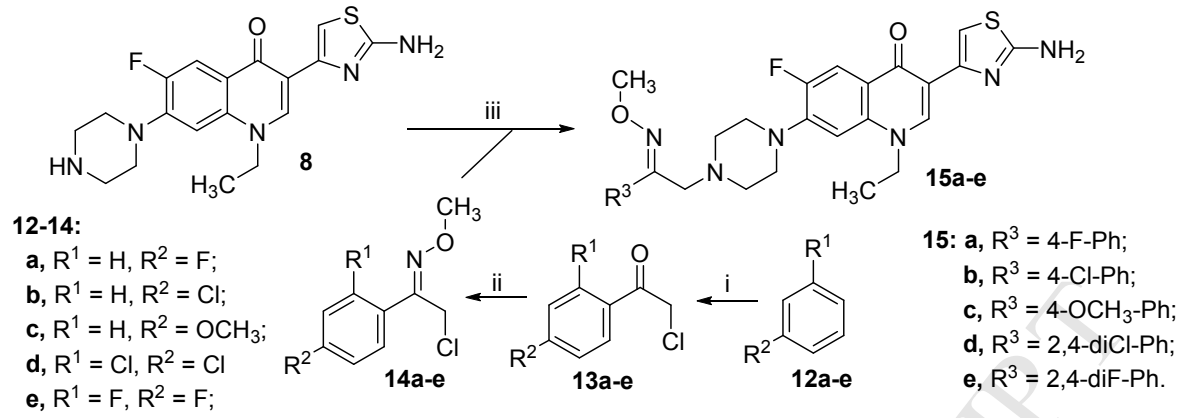

Scheme 2 Synthetic route of 7-substituted aminothiazolquinolone oximes **15a–e**. Reagents and conditions: (i) anhydrous aluminum chloride, chloroacethyl chloride, dichloromethane, r.t., 20 h; (ii) *O*-methylhydroxylamine hydrochloride, EtOH, H_2SO_4, 50 ºC, 4 h; (iii) K_2CO_3, MeCN, 80 ºC, 12 h.

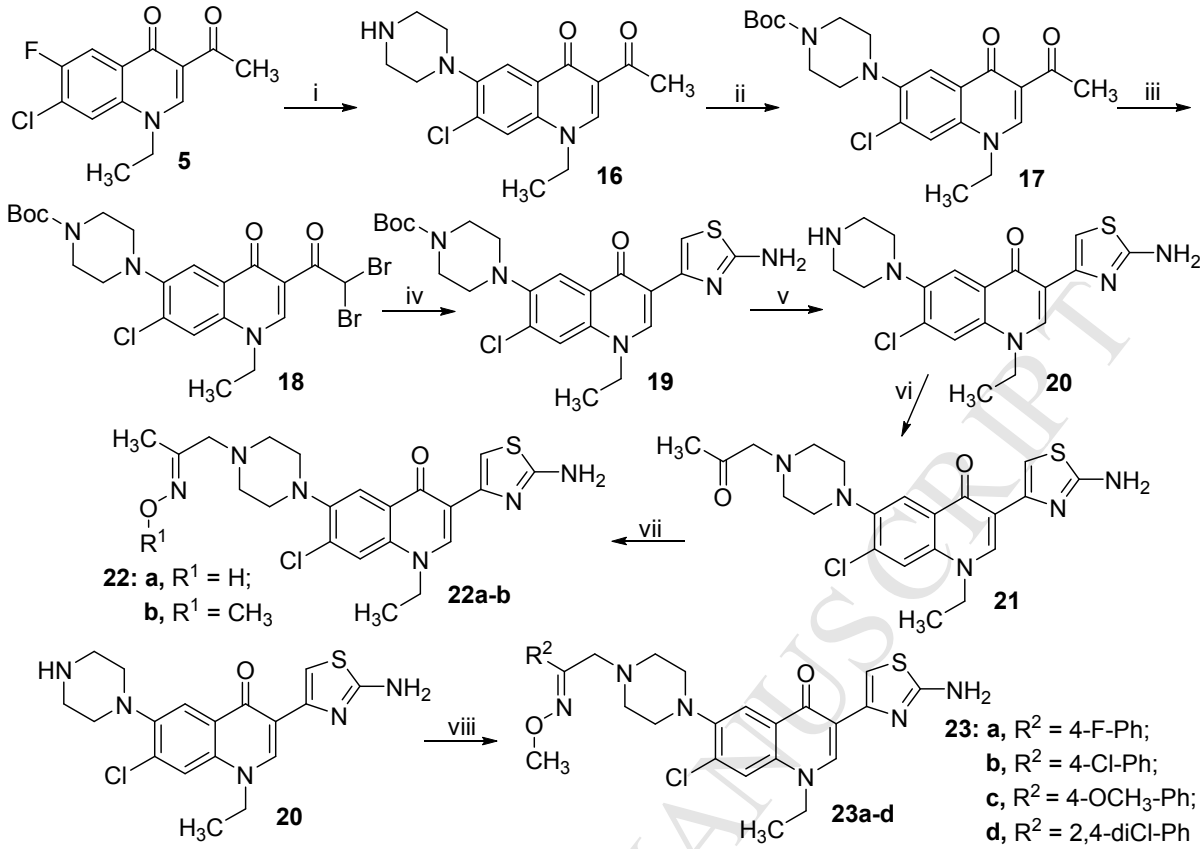

Scheme 3 Synthetic route of 6-substituted aminothiazolquinolone oximes **22a–b** and **23a–d**. Reagents and conditions: (i) piperazine, triethylamine, DMSO, 140 ºC, 12 h; (ii) di-tert-butyl dicarbonate, triethylamine, CH_2Cl_2, r.t., 10 h; (iii) $CuBr_2$, ethyl acetate, 78 ºC, 10 h; (iv) thiourea, EtOH, 80 ºC, 4 h; (v) Con. HCl, CH_2Cl_2, r.t., 2 h; (vi) 1-chloropropan-2-one, K_2CO_3, MeCN, 80 ºC, 10 h; (vii) hydroxylamine hydrochloride or *O*-methylhydroxylamine hydrochloride, K_2CO_3, MeCN, 80 ºC, 10 h; (viii) phenyl *O*-methyl oxime derivatives **14a-d**, K_2CO_3, MeCN, 80 ºC, 12 h.

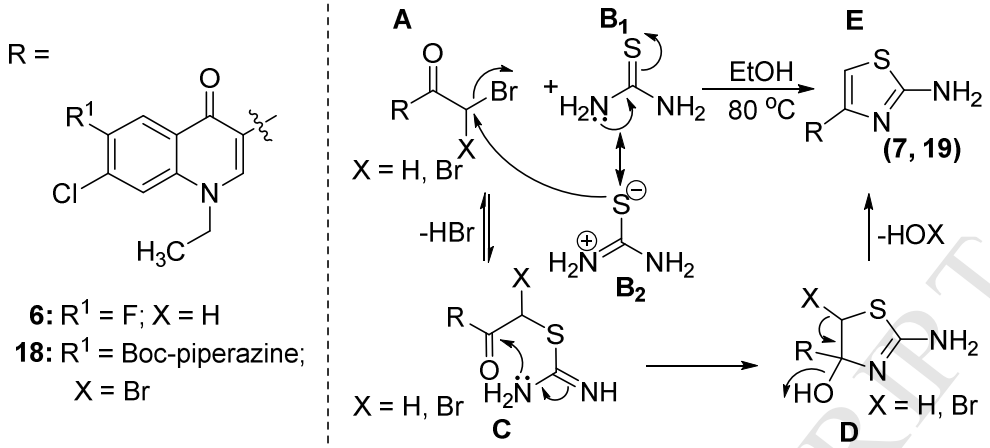

Scheme 4 Proposed mechanism for the construction of thiazole ring (compounds **7** and **19**).

- Novel aminothiazolquinolone oxime derivatives as potentially multi-targeting antimicrobial agents were developed.
- *O*-methyl oxime derivative **10b** displayed excellent inhibitory efficacy against MRSA and *S. aureus* 25923 with MIC values of 0.009 and 0.017 mM, respectively.
- Compound **10b** showed broad antimicrobial spectrum, low toxicity and quite slow development of resistance.
- Molecule **10b** could bind with topoisomerase IV–DNA complex through hydrogen bonds and π-π stacking.
- Compound **10b** could intercalate DNA and bind to human serum albumin.